

1 **Climatic variability over the last 30,000 years recorded in La Piscina de Yuriria, a**
2 **Central Mexican Crater lake (DOI: 10.1002/jqs.2846)**
3
4

5 Jonathan A. Holmes^{1*}, Sarah E. Metcalfe², Heather L. Jones³, Jim D. Marshall⁴.
6

7 ¹ Environmental Change Research Centre, Department of Geography, University College
8 London, Gower Street, London, WC1E 6BT, UK
9

10 ²School of Geography, University of Nottingham, University Park, Nottingham, NG7 2RD,
11 UK
12

13 ³15 Poppy Close, Southwater, Horsham, RH13 9GW, UK
14

15 ⁴ Department of Earth, Ocean and Ecological Sciences, University of Liverpool, Liverpool,
16 L69 3GP, UK
17

18 **Corresponding author:** Jonathan A. Holmes, j.holmes@ucl.ac.uk
19

20 Running head: Palaeolimnology of a Mexican Crater Lake
21

22 **ABSTRACT:** The Trans-Mexican Volcanic Belt provides an excellent setting for
23 reconstruction of late Quaternary climate from different natural archives. Moreover human
24 impact on the landscape since the mid Holocene provides a good opportunity to
25 investigate the complex interplay of natural and anthropogenic forcing of landscape
26 change. However despite the wealth of records, understanding of the environmental
27 history of the region and its wider significance for climate change across the northern
28 neotropics remains incomplete. We present a radiocarbon-dated, multiple-proxy
29 (sedimentology, sedimentary geochemistry, ostracods, diatoms, stable isotopes) record of
30 climatic and environmental change based on the lacustrine sediments from La Piscina de
31 Yuriria, a hydrologically-closed volcanic crater in the northern TMVB. Much of the last
32 glacial interval was characterised by low effective moisture associated with a weakened
33 North American Monsoon (NAM) although the interval from 30,000 to 27,500 aBP
34 experienced abrupt changes in rainfall. The period corresponding to the late glacial stadial
35 was also dry and the lake may have dried out at this time. There was a change to wetter
36 but variable conditions during the early Holocene as the NAM strengthened. Progressive
37 drying during the later Holocene was accompanied by phases of catchment disturbance,
38 which were partly the result of human impact.
39
40
41

42 **KEYWORDS:** Trans-Mexican Volcanic Belt; Palaeolimnology; diatoms; ostracods; stable
43 isotopes
44
45
46
47
48

49 **Introduction and previous work**

50 The highlands of the Trans-Mexican Volcanic Belt (TMVB), which cross Mexico at around
51 19°N, provide a range of opportunities for reconstructing past climates through the study of
52 the sediments in its many lake basins, the availability of glacial deposits, tree ring records
53 and a wealth of historical documents (primarily since the Spanish conquest in 1521). In
54 spite of these many possibilities, understanding of climatic variability over the late
55 Quaternary, particularly the late Pleistocene and early Holocene, is still rather limited
56 (Caballero *et al.*, 2010). A number of factors help to explain this, including poor dating
57 control of many records, the effects of tectonic and volcanic activity, and especially human
58 disturbance, which over at least the last 4000 years has had a profound impact on the
59 natural environment to the extent that only records from the highest elevations may be
60 unaffected (e.g. Lozano-Garcia and Vazquez-Selem, 2005). Lake sediment records have
61 dominated studies of central Mexican palaeoclimatology, although recent speleothem
62 records (Bernal *et al.*, 2011) have also made a contribution. Palynology has played a
63 central role in palaeolimnological investigations dating back to the 1950s (Sears and
64 Clisby, 1995; Watts and Bradbury, 1982; Goman and Byrne, 1998; Lozano-Garcia *et al.*,
65 2005). In this context, the dominance of pine-oak woodlands at higher altitudes in the
66 TMVB has presented further challenges given the limited taxonomic resolution of these
67 pollen types in standard palynology and the impact of long-range dispersal, especially of
68 pine pollen (Correa-Metrio *et al.*, 2012). The climatic interpretation of pollen diagrams
69 from the TMVB has often hinged on decisions about the climatic conditions that changing
70 proportions of pine and oak represent, or indeed whether the presence of large
71 percentages of pine means that pine trees were actually present (c.f. Brown, 1985; Park *et*
72 *al.*, 2010). Pollen records are also highly susceptible to anthropogenic disturbance,
73 although the distinctive presence of *Zea mays* pollen in records is a clear indicator of
74 agricultural activity close to lakes. To help to resolve some of the uncertainties around

75 pollen-based reconstructions, the application of palaeolimnological methods, particularly
76 diatom, geochemical, isotopic and mineralogical analyses, has become increasingly
77 common across the TMVB. Whilst not immune to many of the complicating factors
78 outlined above, this multi-proxy approach has helped to improve our understanding of both
79 climatic and environmental change in this area. In this paper we present a well-dated
80 palaeolimnological record from a crater lake, La Piscina de Yuriria, on the southern edge
81 of the Valle de Santiago region, southern Guanajuato, which extends back some 30,000
82 years (all ages quoted in this paper that relate to the radiocarbon time-span are in
83 calendar years unless otherwise stated). This is considered in the context of other data
84 from adjacent crater lakes in the Valle de Santiago area and other lakes in the wider
85 region to explore the timing and nature of climatic change and human impact.

86
87 The present-day climate of the region, and climate forcing mechanisms over the late
88 Quaternary, are complex. Central Mexico falls under the influence of the North American
89 Monsoon (NAM). Variations in rainfall are forced by northern hemisphere summer
90 insolation over the longer term (millennial timescales) linked to precession, which has
91 caused changes in the position of the inter-tropical convergence zone (ITCZ) (Metcalf *et*
92 *al.*, 2015). On shorter (centennial and shorter timescales), changes in the Pacific and
93 Atlantic Oceans, both of which are important moisture sources, have influenced rainfall
94 over tropical North America and Central America. During the last glacial and first half of the
95 Holocene, the presence of the Laurentide Ice Sheet influenced the climate of the NAM
96 region. The ice sheet had direct effects, through its impact on the position of the jet stream
97 and the mid-latitude westerly winds, and indirectly via meltwater influx into the Gulf of
98 Mexico, a significant moisture source (Aharon, 2003). As the influence of orbitally-forced
99 summer insolation waned over the course of the Holocene, the effect of other factors such
100 as sea-surface temperature variations in the Pacific and Atlantic, linked to various inter-

101 annual modes of ocean-atmosphere re-organisation, has become increasingly important
102 (Metcalf *et al.*, 2015).

103

104 **Study Region**

105 La Piscina de Yuriria lies within the Valle de Santiago, which is located at the northern
106 edge of the Michoacán-Guanajuato Volcanic field (Fig. 1), and is distinctive because of the
107 presence of at least seventeen maar type volcanoes, of which a number contained lakes
108 (Aranda Gomez *et al.*, 2013). It lies on the margin of the volcanic uplands to the south and
109 the lowlands of the Rio Lerma, in an area known as the Bajío, which became a very
110 important agricultural region during the Spanish Colonial period (Butzer and Butzer, 1993).

111

112 Seven maar lakes have been identified around the town of Valle de Santiago, of which
113 four contained water in 1900 (Ordonez, 1900). K-Ar dating of some of the maars puts their
114 formation to between 1.2 Ma (Hoya San Nicolas) and 0.07 Ma (Hoya La Alberca).

115 Unfortunately, the maar that contains La Piscina de Yuriria was not dated, although the
116 adjacent shield volcano is believed to date to 6.9 Ma (Aranda-Gomez *et al.*, 2013). It has
117 been suggested that these maar lakes were once set within a large palaeolake, which
118 extended from the modern Laguna de Yuriria, northwards around the modern town of
119 Valle de Santiago. The maars have very small catchment areas and the lakes within them
120 were supported by the waters of the underlying Salamanca aquifer. Unfortunately, this
121 aquifer has been heavily exploited (there are more than 1600 active wells), which has
122 resulted in a drawdown of about 2 m yr⁻¹ over the past 25 years (Alcocer *et al.*, 2000). As
123 a result all the maars are now dry, even those that contained deep lakes in the early
124 1980s. Alcocer *et al.* (2000) report on the many undesirable consequences of this
125 desiccation, including the loss of endemic fish species and lake margin wetland habitats,
126 the economic effect of the loss of fisheries and alkali fly collection and adverse health

127 effects due to the mobilisation of alkaline dust. La Piscina de Yuriria contained a lake
128 approximately 2 m deep in 1981 and was then observed to dry out through the 1980s, with
129 the development of a salt crust across the basin floor. Freshwater springs around the
130 margins of the lake within the crater also dried up. A shallow lake was re-established in
131 the early 1990s, which was then made permanent in the early 2000s by the pumping of
132 groundwater back into the crater. As this was one of the basins where adverse health
133 effects were reported due to dust mobilisation, this re-wetting of the basin may have been
134 a response.

135

136 The Valle de Santiago area lies towards the northern margin of what was the
137 MesoAmerican cultural area in the pre-Hispanic period. There is limited evidence for
138 settlements during the Preclassic period associated with the Chupicuaro culture (ca. 800 –
139 0 BC). Population expanded during the Classic period (ca. AD 300 – 900) when urban
140 centres developed across the Bajío. In the late Postclassic (after ca. AD 1300) the area
141 lay near the frontier between the settled Purépecha (Tarascans) to the south and the
142 nomadic Chichimec to the north (Gorenstein and Pollard, 1983). A church (convento) was
143 built at Yuririapundaro (the Purépecha name for Yuriria) in 1550. The translation of
144 Yuririapundaro is ‘Lake of Blood’, referring to the distinct red colour of the water in the
145 crater (de Escobar 1729 in Gomez de Orozco, 1972). A similar red colour, probably the
146 result of blooms of sulphur bacteria, was observed at the lake in the 1980s. According to
147 Park *et al.* (2010) the Spanish settled in Valle de Santiago in the early 17th century
148 initiating a period of intensive agricultural exploitation that has lasted until the present day.

149

150 The dramatic effects of water extraction on the maar lakes attracted work on what had
151 been the deep lakes of Hoya la Alberca and the Hoya Rincon de Parangueo (Kienel *et al.*,
152 2009; Park *et al.*, 2010) partly in an effort to retrieve cores of laminated sediments before

153 these became lost through deflation or profoundly disturbed by desiccation and secondary
154 precipitation of evaporite minerals. The Hoya Rincon de Parangueo record goes back to
155 9600 aBP. Prior to this, there had been work on the Hoya San Nicolas (Brown, 1985;
156 Metcalfe *et al.*, 1989), which had been cored in 1979 shortly after it dried out. The basal
157 date on this core was 12,600-12,700 aBP. This maar was re-cored in 2001 with the results
158 reported by Park *et al.* (2010) giving a record believed to extend back to 11,600 aBP (but
159 not directly dated). As described further below, La Piscina de Yuriria was cored in 1981
160 and 1982 prior to its desiccation.

161

162 The interpretation of sequences from the Valle de Santiago maar lakes has been subject
163 to the common uncertainties that affect records from the TMVB region. The interpretation
164 of pine pollen (or the ratio of pine to pine + oak) has been particularly significant here, with
165 Park *et al.* (2010) rejecting Brown's earlier interpretation of wetter conditions between ca.
166 5700 aBP and 3800 aBP in the Hoya San Nicolas. The shallower lakes also seem to have
167 dried up quite regularly through the Holocene, possibly three times in the case of Hoya
168 San Nicolas (Park *et al.*, 2010). The basic framework of change based on these earlier
169 studies seems to be as follows: a cool and relatively moist late glacial (prior to ~12,700
170 aBP); a variable late glacial to Holocene transition; a dry (possibly very dry) early
171 Holocene; the rapid establishment of wetter conditions around 8400 aBP lasting until 5700
172 aBP; dry 5700 – 3800 aBP, then wetter again, but not as wet as the period between
173 around 8400 and 6000 aBP. The late Holocene has been profoundly influenced by human
174 activity with evidence of maize cultivation and enhanced erosion (especially 2200 to 1300
175 aBP). Both Metcalfe *et al.* (1989) and Park *et al.* (2010) report a cessation of human
176 disturbance around 1000 aBP followed by renewed activity after 400 aBP probably
177 associated with Spanish settlement. Our new data from La Piscina de Yuriria allow us

178 both to extend this record back into the last glacial and to test the framework outlined
179 above.

180

181 **Study site**

182 This study is based on lake sediment records from La Piscina de Yuriria (20°30'N;
183 101°08'W, 1740 m a.s.l), which is one of the small (area = 0.75 km²), hydrologically-closed
184 maar lakes in the Valle de Santiago region (Fig. 1). The basaltic basin experiences a
185 subhumid, subtropical climate with annual precipitation of 700-800 mm and supports
186 subtropical thorn bush scrub around the lake and sparse oak woodland above 2200 m
187 a.s.l. (Metcalf and Hales, 1994; Metcalfe *et al.*, 1994). The lake seems to have been
188 generally shallow in recent times (e.g. ~ 2 m deep in 1981 and 1982, <1 m in 1992, >1.8
189 m in 2004) and has dried up totally in some years (e.g.1989). The lake was saline as a
190 result of evaporative enrichment, as well as highly eutrophic, with an alkalinity/Ca ratio >>1
191 and Na-CO₃-Cl-type composition indicating that evaporative evolution occurred along
192 pathway IIIA of Eugster and Hardie (1978). The lake was fed by several circum-neutral to
193 alkaline springs that were fresh to slightly brackish (Table S1) and also of Na-HCO₃ type.
194 Evaporative enrichment is also reflected in the limited stable isotope data for the input
195 water (-9.2 ‰) versus lake water (+0.7 ‰) (Table S1). Recent water-level changes have
196 been the result of groundwater extraction for irrigation (e.g. Metcalfe and Hales, 1994) and
197 later artificial recharge; variations during the late Quaternary, which form a major focus of
198 the present study, have largely been driven by changes in effective moisture (precipitation
199 minus evaporation, or P-E), as discussed below.

200

201 **Materials and methods**

202 *Field collection*

203 Two lake sediment cores, namely cores YC1 (length 4 m) and YC2 (14.3 m), were
204 recovered from La Piscina de Yuriria from under 2 m of water in 1981 and 1982,
205 respectively, by members of the Tropical Palaeoenvironments Research Group, at the
206 time based at the University of Oxford, UK. Cores were initially wrapped in clingfilm and
207 aluminium foil and stored in plastic tubes at 4 °C prior to sectioning into 1 cm slices,
208 typically at 5 cm intervals, for analysis. Some of the data for core YC1 have been
209 published previously (Metcalf and Hales, 1994; Metcalfe *et al.*, 1994) but are summarised
210 here alongside previously unreported data for that core and for YC2.

211

212 *Physical sedimentology*

213 Sediment samples from YC1 and YC2 were analysed for organic carbon content using
214 loss on ignition at 450 °C, and for carbonate content by calcimetry. Low-frequency
215 magnetic susceptibility was measured using a Bartington MS1 magnetic susceptibility
216 meter.

217

218 *Bulk sediment geochemistry*

219 Dried sediment samples from YC1 were digested using a combination of HNO₃, HF and
220 H₂O₂ following Dean and Gorham (1976). The resulting residue was taken up in dilute HCl
221 prior to analysis of major and minor metals using atomic absorption spectrophotometry
222 (AAS). Samples from YC2 were prepared using the sequential digestion method of
223 Engstrom and Wright (1984) and each separate fraction analyses for major and minor
224 metals as for YC1. However, initial inspection of the results indicated that the fractionation
225 had not worked well for these complex sediments. Consequently, the results for the
226 separated fractions were summed and the data treated as 'bulk' analyses, as for YC1.
227 Only selected metals are reported here, namely Fe, Mn, Al, and K, all of which are

228 abundant in catchment soils and sediments, and so are regarded as good tracers of
229 inwash, as discussed in further detail below.

230

231 *Stable isotopes in endogenic carbonate*

232 Bulk, dried sediment samples from YC1 were sieved through an 80µm mesh to remove
233 shell material, treated with Clorox to remove organic carbon and then dissolved in 100 %
234 phosphoric acid. The evolved CO₂ was then analysed for oxygen and carbon isotopes
235 using a VG 'Micromass' mass spectrometer at the Laboratoire d'Hydrologie et de
236 Géochimie Isotopique, Université de Paris-Sud. Samples from YC2 were prepared in a
237 similar way and analysed using a modified SIRA mass spectrometer at the University of
238 Liverpool. All stable isotope results are reported in standard delta notation relative to the
239 PDB standard.

240

241 As part of the evaluation of the stable isotope results, the mineralogy of the carbonate
242 fractions was assessed by X-ray diffraction using Phillips PW1320/10 and PW1050 X-ray
243 diffractometers. Specifically, the Mg content of calcite was assessed using the method of
244 Goldsmith *et al.* (1961)

245

246 *Ostracods*

247 Bulk sediment samples were disaggregated in ~5 % H₂O₂, sieved through a 63 µm sieve
248 and the coarse fractions used for extraction of ostracod shells under a low-power binocular
249 microscope. Because ostracod abundance varied dramatically, in some samples all of the
250 ostracod valves were picked whereas in richer samples, only the first 350 valves were
251 picked and overall abundance then estimated based on the weight of sediment examined.
252 However, the unpicked fraction of rich samples was inspected for the presence of rare
253 species not identified in the original count. Despite poor ostracod shell preservation in

254 many parts of the core, sufficiently well-preserved valves were found at a number of levels
255 to permit stable-isotope analyses, which were used to complement analyses on the
256 endogenic carbonate.

257

258 Specimens of ostracods from the picked fraction of YC2 were selected and studied
259 carefully for signs of damage, dissolution or replacement. Suitable individuals were then
260 cleaned carefully using a 000 size clean nylon paintbrush and ultra pure deionised water
261 under a binocular microscope to remove surface contaminants. Stable-isotope analyses of
262 multiple shells of *Limnocythere sappaensis* were analysed for oxygen and carbon isotopes
263 using a VG Isocarb coupled to a VG Optima mass spectrometer at the NERC Isotope
264 Geosciences Laboratory, Keyworth (UK). Two samples, composed of up to 8 individual
265 valves, were analyzed at most core levels selected and a weighted mean value for $\delta^{18}\text{O}$
266 and $\delta^{13}\text{C}$ calculated for plotting purposes.

267

268 *Diatoms*

269 Diatom samples were prepared for analysis at 10 cm intervals in YC1 and 10 – 20 cm
270 intervals (depending on sample availability) in YC2. In YC2, only material from 4 m to the
271 base was sampled in detail after preliminary analysis (samples prepared every 25 – 30
272 cm) had shown that the upper 4 m of the sequence seemed to match well with YC1. Poor
273 valve preservation between 7 m and 12 m meant that the majority of samples were taken
274 below and above this interval. Core samples were complemented by a surface sediment
275 sample and water samples from the lake margin. Samples were treated to remove
276 carbonates and organic matter following the method of Battarbee (1986). In some cases
277 strong acids (H_2SO_4 or HNO_3) were used to break up clumps of sediment. The final
278 suspension was mounted onto coverslips using Naphrax. The same method was used to
279 prepare surface sediment samples. Where possible, 400 valves were counted from each

280 level, although at levels with poor preservation this was sometimes reduced to 100 – 200
281 valves. Identifications were carried out using standard floras including Gasse (1986),
282 Krammer and Lange Bertalot (1988, 1991a and b), Patrick and Reimer (1966, 1975),
283 Schoeman and Archibald (1977). The separation of *Navicula (Craticula) elkab* from
284 *Craticula halophila* proved to be an important part of the study and is discussed in
285 Metcalfe (1990). The results from YC1 were published in Metcalfe and Hales (1994), and
286 preliminary results from YC2 were described in Park (1999). Diatom results are presented
287 here as percentages of the full counts. Species present at less than 2% and only
288 occurring in one sample are not plotted here.

289
290 Initial zonation was carried out using CONISS, the stratigraphically constrained cluster-
291 analysis program within Tilia (Grimm, 1987). The counts from the core samples were also
292 analysed using CANOCO and TWINSPAN. TWINSPAN (Hill, 1979; Jongman *et al.*, 1992)
293 provided a clustering that was not constrained stratigraphically. CANOCO (ter Braak,
294 1988) was used to explore further the variation between samples and species. The latter
295 analyses were used to determine whether the lake diatom assemblages showed repeat
296 occurrences through time and to explore that trajectory of change.

297

298 *Chronology*

299 Independent chronologies were established using AMS or radiometric radiocarbon dating
300 on bulk organic carbon or carbonate (8 levels were dated from YC1 and 16 from YC2).
301 Lack of appropriate material precluded the dating of terrestrial plant macrofossils from
302 either core, but the absence of carbonate bedrock within the catchment means that
303 hardwater error is unlikely to affect radiocarbon dates at this site. Radiocarbon
304 measurements were performed at the Oxford University Radiocarbon Accelerator Unit,
305 Simon Fraser University Radiocarbon facility, Laboratoire d'Hydrologie et de Géochimie

306 Isotopique, Université de Paris-Sud, the NERC Radiocarbon Facility, East Kilbride and the
307 Arizona AMS Laboratory, University of Arizona. Dates were calibrated using IntCal13
308 (Reimer *et al.*, 2013). For each core, outliers were identified and excluded from
309 subsequent age modeling, which was undertaken using Clam 2.2 (Blaauw, 2010).
310 Although some of the radiocarbon dates have been published previously, we report them
311 again here for the sake of completeness and because we have revised the calibrations.

312

313 **Results**

314 *Chronology*

315 The age model for YC1 is based on 7 of the 8 radiocarbon dates for that core (Table 1,
316 Fig. 2) and the age-depth pairs well described by a 3rd-order polynomial curve. The age
317 model for YC2 is based on 12 of the 16 radiocarbon dates (Table 1, Fig. 2) and the age-
318 depth pairs well described by a 3rd-order polynomial curve. The age models were used to
319 assign ages to each depth within the respective cores. An assessment of the comparability
320 of the independent age models for YC1 and YC2 was also undertaken by comparing
321 variations in their physical sedimentology, which would be expected to change
322 synchronously in the two cores: this assessment is discussed below.

323

324 *Physical sedimentology*

325 Cores YC1 and YC2 core are both composed predominantly of brown to grey,
326 diatomaceous gyttja. In the lower sections of YC2 (at ~26,300, 19,900 and 8300 aBP),
327 centimetre-scale sand layers are present. Desiccation surfaces, represented by sub-
328 vertical fractures infilled with darker material, occur at several depths in the interval
329 between 16,800 and 14,300 and near the top of the sequence (~800 aBP). Nodular,
330 siliceous concretions were observed between the base of the sequence and ~17,500 aBP.
331 The interval 100 – 50 cm (representing ~1100 – 500 aBP) was not recovered in YC2.

332

333 Organic carbon content, estimated from loss-on-ignition (LOI) at 450°C, varies between ~9
334 and 44 % (Fig. 3). From the beginning of the YC2 record until ~14,000 aBP, values
335 average ~15%, increasing and becoming more variable after this time, with peaks up to 44
336 %. The LOI record in the upper part of YC2 is well replicated in YC1. Carbonate content
337 averages around 18 % from the beginning of the record until 14,200 aBP, but with peaks
338 up to 40 % in places. Between 14,000 and 7800 aBP, carbonate content falls to 14 % and
339 becomes less variable. From 7800 aBP to the end of the YC2 record, there is a sharp
340 increase to an average of 33 %, with transient peaks up to 45 %. The pattern of change in
341 YC1 replicates that in the upper part of YC2, but values are systematically lower.

342

343 Magnetic susceptibility (χ) values (Fig. 3) are typically lower than $10 \times 10^{-7} \text{m}^3 \text{kg}^{-1}$ but with a
344 number of sharp peaks at several levels and a more gradual increase and then decline
345 between ~10,100 and 6900 aBP. Values rise sharply at 3600 aBP, after which they remain
346 high and show increased variability. The pattern of change in YC1 replicates that in the
347 upper part of YC2.

348

349 *Geochemistry and stable isotopes*

350 Concentrations of K, Fe, Mn and Al are variable throughout the cores. For much of the
351 lower part of YC2 values are generally low, although there are some transient peaks.

352 Values typically become higher and more variable after about 5100 aBP in YC2, a pattern
353 that is generally replicated in YC1. There is strong and statistically-significant correlation
354 amongst all of the metals discussed here in YC1 and in the section of YC2 covering the
355 past ~5000 years. Correlations are weaker for the earlier part of YC2 (Table S2).

356

357 Stable isotope values are available for fine-grained carbonates and, for a few levels from
358 YC2 only, for ostracod shells (Fig. 4). Mineralogical determinations showed that the calcite
359 present within the core had low magnesium content (≤ 4 mole %): nevertheless,
360 appropriate corrections were made to the $\delta^{18}\text{O}$ values following Tarutani *et al.* (1969).
361 From the beginning of YC2 to 26,600 aBP, $\delta^{18}\text{O}$ and $\delta^{13}\text{C}$ values are typically low but
362 variable (from about 0 ‰ to around -11 ‰ and +7.6 to -1 ‰, for $\delta^{18}\text{O}$ and $\delta^{13}\text{C}$,
363 respectively) and strongly covariant (Fig. 5). Between 25,000 and 14,200 aBP, the stable-
364 isotope values are at relatively low resolution, and typically values are higher than in the
365 preceding interval (up to about +3 ‰ and +8 ‰ for $\delta^{18}\text{O}$ and $\delta^{13}\text{C}$, respectively) and
366 covariant. Between 10,900 and 6600 aBP, there is a further rise in variability, but $\delta^{18}\text{O}$ and
367 $\delta^{13}\text{C}$ covary as before. Between 6600 and 4500 aBP, there is a significant shift in the
368 pattern of stable isotope variability, with $\delta^{18}\text{O}$ values remaining relatively constant, but $\delta^{13}\text{C}$
369 increasing up to +15.4 ‰. After 4500 aBP, $\delta^{18}\text{O}$ values vary between about 0 and -2.7 ‰
370 and $\delta^{13}\text{C}$ values are markedly reduced compared with the preceding interval. The
371 overlapping sections of YC1 and YC2 show similar patterns of change, especially for $\delta^{13}\text{C}$.
372 The low-resolution ostracod values are typically ^{18}O -enriched and ^{13}C -depleted compared
373 with those for fine-grained carbonates.

374

375 *Ostracods*

376 Ostracod abundance varies dramatically, between zero (i.e. barren levels) and ~35,000
377 valves per gram of sediment (Fig. 4). Significant zones of very high abundance are
378 present from the beginning of the YC2 record to until 28,700 aBP and at 21,900 – 21,300
379 aBP, 17,800 – 15,900 aBP, 13,700 – 12,900 aBP, 4800 - 2700 aBP, 2000 – 1100 aBP.
380 Significant zones that are barren or contain very few ostracods occur at 28,500 – 27,800
381 aBP, 19,000 – 18,500 aBP, 15,400 – 14,400 aBP, 10,500 – 8300 aBP, 5300- 4900 aBP.
382 The zones of high abundance generally contain monospecific assemblages of

383 *Limnocythere sappaensis* (both males and females): zones of lower abundance typically
384 support other species as well, including at least one species of candonid, *Heterocypris* sp.,
385 *Physocypris* sp., *Potamocypris* sp., *Strandesia* sp. and *Cyprina* sp. Although *L. sappaensis*
386 is regarded as conspecific with *Limnocythere inopinata* (e.g. Martens, 1994), we adopt the
387 name *L. sappaensis* here since this is widely used for the species in North America.

388

389 *Diatoms*

390 The diatom assemblages from surface sediment samples collected in 2 m of water in 1982
391 were dominated by *Navicula (Craticula) elkab* (22%), *N. (C.) halophila* (13%) and a variety
392 of *Nitzschia* species. A sample taken in 1997 in 0.3 m of water, just as a lake was
393 becoming re-established, was dominated by *Anomoeoneis sphaerophora* (48%) and
394 *Navicula (Craticula) elkab* (16%). *Anomoeoneis costata* and *Chaetoceros muelleri* spores
395 made up 8% of the count each (Davies, 2000). A sample taken in 2004, at the edge of the
396 lake, was dominated by *Navicula (Craticula) halophila* (56%), a range of *Nitzschia* species,
397 *Chaetoceros muelleri* (some as resting spores) and *Anomoeoneis sphaerophora* f.
398 *costata* (Hill, 2006), although these each formed less than 6% of the assemblage. In 2004,
399 the lake was hypereutrophic, with TP = 584 $\mu\text{g l}^{-1}$ and chlorophyll-a 127 $\mu\text{g l}^{-1}$ (Hill, 2006).

400

401 Preliminary diatom analysis of samples from the top 4 m (past ~5000 years) of the YC2
402 core indicated the presence of similar assemblages to those reported in Metcalfe and
403 Hales (1994), so efforts on this core were focused on the section below 4 m. Here, results
404 are presented from both core sequences (Fig. 6). As with the ostracods, diatom
405 preservation is highly variable through the sequences. In YC2 there was little or no valve
406 preservation between 22,100 – 10,400 aBP cm. In YC1 there are gaps in the record due
407 to poor preservation between 2000 – 1100 aBP. Both sequences are dominated by *N. (C)*
408 *halophila* and *N. (C) elkab*, *A. costata* and *A. sphaerophora*, *C. muelleri* and a range of

409 *Nitzschia* species. These assemblages are all similar to those found in surface sediment
410 samples taken from the lake at different times, reflecting high (if varying) pH and alkalinity,
411 and highly evaporated conditions. A more distinctive aspect of the core records is the
412 abundance, at times, of small *Navicula* species (e.g. *N. fluens*, *N. minusculoides*, *N.*
413 *muralis*).

414

415 **Discussion**

416 We discuss the chronology for the lake-sediment sequences and then the interpretation of
417 each of the palaeolimnological variables, before proceeding to reconstruct the
418 palaeolimnological history of La Piscina de Yuria for the late Quaternary.

419

420 Core YC1 covers the interval from about 4600 aBP to the coring date. The anomalous age
421 at 44-46 cm probably represents inwash of older carbon from the catchment, substantiated
422 by the magnetic susceptibility data. Core YC2 covers the interval from about 31,000 aBP
423 to the coring date. The four dates that are omitted from the age model are all younger than
424 expected, possibly the result of root penetration during times of low lake level. The general
425 pattern of age-depth relationships for YC1 and the upper part of YC2 suggests good
426 agreement between the two cores. Detailed comparisons based on the loss on ignition
427 and magnetic susceptibility profiles (Fig. 2), which would be expected to agree for the two
428 closely-located sequences, suggest a small (~200 years) age offset, with YC2 being
429 consistently older. The fact that small differences exist is perhaps not surprising given that
430 different equivalent depths and contrasting materials were dated in the two cores (Table
431 1). However, rather than correct either one of the cores we prefer to use the age models
432 defined for each respective core and then refer to the resulting uncertainties as
433 appropriate.

434

435 Loss on ignition (LOI) provides a good proxy for the organic carbon content of the
436 sediments (Dean, 1974). The carbon/nitrogen (C/N) ratios (available for YC1 only: data not
437 shown, but values vary between 11.6 and 49.4) indicate that the organic matter is of mixed
438 aquatic and terrestrial sources, suggesting that LOI provides a record of aquatic
439 productivity and terrestrial inwash at least for the past 4,600 years. The CaCO₃ content of
440 the sediment is best explained by endogenic carbonate formation within the lake, since the
441 catchment is devoid of carbonate rocks or sediments. In such settings, calcium carbonate
442 precipitates from the water column when the lake becomes saturated with respect to
443 carbon minerals as a result of evaporative enrichment of water or mediated by aquatic
444 plants. However, enhanced aquatic productivity can also lead to carbonate dissolution
445 (e.g. Cohen, 2003) and carbonate formation also depends on supply of ions from the
446 catchment, meaning that the interpretation of sedimentary CaCO₃ records is not always
447 straightforward.

448

449 The magnetic susceptibility of the sediments is strongly linked to inwash because the
450 volcanic soils are rich in magnetic minerals. Increases in χ in YC1 have therefore been
451 interpreted as inwash events associated with either natural or anthropogenic catchment
452 disturbance (Metcalf and Hales, 1994). The elements Fe, Mn, Al and K are all associated
453 with weathered volcanic soils, and their concentrations in the lake sediments are
454 controlled by catchment inwash: Fe and Mn may also have been mediated by redox
455 conditions within the lake although we do not have direct evidence for this.

456

457 The oxygen and carbon isotope composition of lacustrine carbonate is a function of the
458 temperature and isotopic composition of the water in the case of oxygen, and the carbon-
459 isotope composition of dissolved inorganic carbon (DIC) for carbon. In subtropical dryland
460 lakes, such as La Piscina de Yuriria, the oxygen-isotope ratio of lake water is usually the

461 dominant control on the oxygen-isotope composition of carbonate, and this varies with the
462 degree of evaporative enrichment (Talbot, 1990). The carbon-isotope composition of DIC
463 is a complex function of carbon source (catchment- vs lake-derived) and in-lake
464 modification as a result of fractionation during DIC uptake by aquatic plants for
465 photosynthesis, and exchange with atmospheric CO₂ (Talbot, 1990) The same general
466 controls determine the isotopic values of biogenic carbonates, such as ostracod shells, but
467 there may be taxon-specific differences in the exact location and timing (especially
468 season) of carbonate formation compared with endogenic carbonate (e.g. Decrouy *et al.*,
469 2011). Moreover, biogenic carbonate may not be precipitated in isotopic equilibrium with
470 lake water or DIC: ostracod shells, for example, demonstrate offsets from oxygen-isotope
471 equilibrium and are typically ¹⁸O-enriched compared with endogenic carbonate
472 precipitated in equilibrium with lake water (von Grafenstein *et al.*, 1999). Further
473 palaeolimnological inferences can be drawn for the strength of covariance amongst
474 carbonate oxygen and carbon isotope values in sediment sequences, strong covariance
475 typically being associated with hydrologically-closed systems (Talbot, 1990).

476
477 Although the occurrence and abundance of different lacustrine ostracod taxa are
478 determined by a range of factors, in La Piscina de Yuriria, salinity, hydrochemistry and the
479 extent to which the lake is seasonally permanent are likely to be the dominant controls. In
480 saline lakes, there is moreover often a relationship between species diversity and ostracod
481 abundance: highly saline lakes are typically dominated by a single species that is present
482 in very high abundance (De Deckker and Forester, 1988).

483
484 Habitat, pH, conductivity, ionic composition and nutrient levels are all major controls on the
485 presence and abundance of diatom species, with some species having well established
486 preferences in relation to some, or all, of these factors (e.g. Gasse, 1986; Kilham *et al.*,

487 1986). In La Piscina de Yuriria, the dominant controls over the full record appear to be
488 those associated with changes in evaporative concentration (pH, EC, ionic composition).
489 NaCl and Na₂CO₃ waters have been shown to be particularly aggressive in relation to
490 diatom dissolution (Barker *et al.*, 1994), so it is likely that some species may be over-
491 represented in the sediment record due to their robust form and heavy silicification. This
492 seems particularly likely in the case of the cysts of *C. muelleri* and may also apply to the
493 more robust forms of species such as *A. costata*, *Denticula elegans* and *Rhopalodia*
494 *gibberula*. Although the impact of differential preservation needs to be borne in mind when
495 interpreting the fossil record, saline-lake diatoms are well established as indirect tracers of
496 climate change (Gasse *et al.*, 1997).

497

498 From the base of YC2, which dates to a little before 30,000 aBP, until around 27,500 aBP,
499 the $\delta^{18}\text{O}_{\text{carb}}$ record shows marked variability, with the lowest values equivalent to the
500 minimum for the sequence as a whole, and the highest values close to the maximum (Fig.
501 4). There is strong covariance between $\delta^{18}\text{O}_{\text{carb}}$ and $\delta^{13}\text{C}_{\text{carb}}$ (Fig. 5) consistent with a
502 hydrologically-closed lake undergoing temporal variations in the degree of evaporative
503 enrichment (Talbot, 1990) in response to changes in effective moisture. The most negative
504 $\delta^{18}\text{O}_{\text{carb}}$ values equate to un-evolved lake water that was probably fed by springs and
505 rainfall with lower $\delta^{18}\text{O}$ than at present ($\delta^{18}\text{O}$ around -9 ‰ in summer 1992: Table S1),
506 possibly coupled with cooler conditions. In contrast, the most positive $\delta^{18}\text{O}_{\text{carb}}$ values in this
507 interval are best explained by evaporative enrichment under reduced effective moisture.
508 The lowest $\delta^{13}\text{C}_{\text{carb}}$ can be explained by equilibration with atmospheric CO₂ whereas the
509 more positive values require other, or additional, mechanisms to explain them. The uptake
510 of ¹²C during aquatic photosynthesis by aquatic macrophytes or algae can lead to an
511 increase in the $\delta^{13}\text{C}_{\text{DIC}}$ and hence of endogenic carbonates, but such an explanation
512 appears inconsistent with low TOC values in this interval (Fig. 3). An alternative

513 explanation is the formation of co-genetic, ^{13}C -enriched, CO_2 during methane formation.
514 Despite the evidence pointing to low lake levels at this time, methane formation in shallow
515 and eutrophic lakes has previously been reported in Mexico (Lake Pátzcuaro: Metcalfe *et*
516 *al.*, 2007) and elsewhere (e.g. Lamb *et al.*, 2000; Gu *et al.*, 2004). The high concentrations
517 of *L. sappaensis* in this interval are consistent with the existence of a saline-alkaline lake
518 (Forester, 1986): interestingly, the peaks in ostracod abundance coincide broadly with the
519 peaks in $\delta^{18}\text{O}_{\text{carb}}$, suggesting that ostracod numbers increased with salinity, and hence
520 evaporative enrichment. The occurrence of siliceous nodules within the interval,
521 associated with the levels that have the highest $\delta^{18}\text{O}_{\text{carb}}$ values, is also consistent with the
522 existence of highly saline and alkaline water. The sporadic isotope values from ostracod
523 shells in this interval show ^{18}O -enrichment compared with endogenic carbonates that is
524 broadly consistent with the approximate +0.7 ‰ vital offset recorded for the genus
525 *Limnocythere* (von Grafenstein *et al.*, 1999). In contrast, the carbon isotope values in
526 ostracod shells are similar to those in endogenic carbonate, suggesting that both sources
527 of carbonate precipitated from DIC with a similar $\delta^{13}\text{C}$ value once allowance has been
528 made for differences in the timing and exact location of formation. This period covers
529 diatom zones YC2-I and part of YC2-II (Fig. 6). The base of the core is dominated by *C.*
530 *muelleri*, a diatom known to inhabit chloride-rich waters, but the other taxa here do not
531 indicate hypersaline conditions, so it may be over-represented. The most negative $\delta^{18}\text{O}_{\text{carb}}$
532 value may be reflected in the increase in the freshwater *N. molestiformis* and *N. fluens*
533 although the diatom assemblage overall continues to indicate shallow and alkaline
534 conditions. The presence of *Nitzschia palea* and a form of *Nitzschia frustulum* (both
535 obligate N heterotrophs) also indicates eutrophic conditions, which may help to explain
536 methanogenesis in shallow water conditions (see above). The increasing abundance of *N.*
537 *elkab*, and species of *Anomoeoneis* indicate more consistently high pH (> 8.5) and
538 alkalinity, probably associated with shallowing of the lake. Low magnetic susceptibility and

539 low concentrations of 'inwash' indicator elements (Fe, Mn, K and Al) in this interval
540 suggest that inwash of soil into the lake was limited despite the intervals of increased
541 effective moisture (Fig. 3).

542

543 Between ~27,500 and 14,000 aBP, there was a shift to more positive $\delta^{18}\text{O}_{\text{carb}}$ and $\delta^{13}\text{C}_{\text{carb}}$
544 values, although with some stratigraphical variability and strong covariance between
545 $\delta^{18}\text{O}_{\text{carb}}$ and $\delta^{13}\text{C}_{\text{carb}}$ (Fig.4, Fig. 5). The elevated $\delta^{18}\text{O}_{\text{carb}}$ values suggest enhanced
546 evaporative enrichment of lake water under conditions of low effective moisture: the
547 presence of siliceous nodules at various points in this interval support the argument that
548 the lake was shallow, saline and strongly evaporated. Short-term variations in carbonate
549 content also support the occurrence of strong but variable evaporative enrichment (Fig. 3).
550 The presence of multiple surfaces that probably resulted from desiccation in the later part
551 of this interval suggests that lake levels fell and the lake may have dried out totally on
552 several occasions. Elevated $\delta^{13}\text{C}_{\text{carb}}$ values are too high to be explained solely by
553 equilibration with atmospheric CO_2 . Enhanced aquatic productivity, in which ^{12}C -uptake by
554 aquatic plants and algae causes DIC to be enriched in ^{13}C , is incompatible with the low
555 TOC content in this interval: the production of ^{13}C -enriched co-genetic CO_2 in a stagnant,
556 shallow, nutrient-rich lake could provide an alternative explanation as discussed above.

557 From 27,500 to 22,500 aBP, a period of evaporative enrichment and periodic desiccation
558 is consistent with the diatom record for this interval (zones YC2-IIa and YC2-IIb), which
559 ends around 22,500 aBP in a period when diatoms were sparse and poorly preserved
560 (after which there is a break in diatom preservation, see above). There are two notable
561 peaks in *N. minusculoides* reaching 71% of the count between 27,000 and 26,000 aBP
562 and 44% at around 24,000 aBP. The earlier peak is associated with a layer of sand (or
563 tephra, see below) and, moreover, there are no stable isotope data from this layer, so its
564 significance remains unclear. The presence of some freshwater taxa (e.g. *N. fluens*,

565 *Caloneis bacillum*) may reflect fluctuating conditions within a period of overall drying.
566 There are several marked peaks in ostracod abundance during this interval, with
567 assemblages strongly dominated by *Limnocythere sappausensis*, which supports the
568 inference that the lake was generally saline and alkaline. The sporadic occurrence of other
569 taxa suggests the periodic influx of fresher waters: rather than whole-lake freshening,
570 these taxa could indicate surface or subsurface inflow of fresh water at various times. Low
571 magnetic susceptibility values and low concentrations of 'inwash' elements suggest limited
572 transfer of soil or sediment from the catchment during this interval; two sharp peaks in
573 magnetic susceptibility around 26,000 and 23,000 aBP (Fig. 3) may represent tephra,
574 rather than catchment inwash, although this remains to be confirmed.

575

576 There is a gap in the stable isotope record between 14,000 and 11,000 aBP, but evidence
577 for dry conditions during this interval comes from the presence of a desiccation surface
578 and the occurrence of a possible palaeosol. It is also supported by the lack of diatom
579 preservation. Sporadic ostracod occurrence also suggests that the lake may have been
580 ephemeral during this time. This interval covers the northern hemisphere late glacial
581 stadial event and confirms that this was a time of low effective moisture in central Mexico.

582

583 After 11,000 aBP, there was a shift to more negative and also more variable $\delta^{18}\text{O}_{\text{carb}}$ and
584 $\delta^{13}\text{C}_{\text{carb}}$ values, consistent with a general increase in effective moisture during the early
585 Holocene (Fig. 4). The rise in magnetic susceptibility, coupled with minor increases in
586 some of the 'inwash' elements, may also reflect enhanced inwash of catchment material
587 during the early Holocene. Diatom preservation resumes (zone YC2-III), with assemblages
588 dominated by *Nitzschia palea* and *Chaetoceros muelleri* (Fig. 6). Assuming that *C.*
589 *muelleri* may be overrepresented, high percentages of *N. palea* and *Nitzschia communis*
590 indicate lower pH and TDS (total dissolved solids) (Gasse, 1986) and eutrophic conditions.

591 This assemblage shows some similarities to that in zone YC2-Ia, but zone YC2-III may
592 represent the period when the lake was freshest and deepest, although not deep enough
593 to develop a truly planktonic flora. Today, assemblages with such high percentages of *N.*
594 *palea* are found in shallow, freshwater lakes in Mexico with high levels of nutrient
595 enrichment such as Lakes Zacapu and Cajititlan (Hill, 2006 and S. Metcalfe, unpublished
596 data). Ostracod concentrations are low, but significantly the assemblages include a
597 relatively high proportion of species other than *L. sappaensis*, consistent with fresher
598 water than in much of the pre-Holocene.

599

600 Between about 8,000 and 4,500 aBP there was a marked change in the lake system.
601 Increase in $\delta^{18}\text{O}_{\text{carb}}$ values suggests enhanced evaporative enrichment associated with
602 decreased effective moisture (Fig. 4). Most notably, however, is the dramatic positive
603 excursion in $\delta^{13}\text{C}_{\text{carb}}$ values, up to a maximum of about +16 ‰ and, associated with this,
604 the breakdown in the positive covariance between $\delta^{18}\text{O}_{\text{carb}}$ and $\delta^{13}\text{C}_{\text{carb}}$ values that was
605 apparent during earlier intervals (Fig. 5). The very high $\delta^{13}\text{C}_{\text{carb}}$ values are best explained
606 by methanogenesis, as discussed for earlier intervals above. Interestingly, the single
607 $\delta^{13}\text{C}_{\text{ostracod}}$ value from this interval does not track the $\delta^{13}\text{C}_{\text{carb}}$ values, but instead is much
608 lower (Fig. 4). Although we cannot attach too much significance to a single value, this
609 does suggest that the ostracods and the endogenic carbonate were formed in different
610 micro-environments within the lake, or perhaps during different seasons, from DIC with
611 contrasting $\delta^{13}\text{C}$ values. Although the $\delta^{18}\text{O}_{\text{ostracod}}$ values are more positive than the $\delta^{18}\text{O}_{\text{carb}}$
612 values, as would be expected, the difference is too large to be explained by vital offsets
613 alone, possibly lending support to the view that the endogenic and ostracod carbonates
614 were formed under contrasting conditions or at different times of the year. Ostracods occur
615 sporadically in this interval, indicating that whatever conditions prevailed were not wholly
616 unsuitable for ostracods to live. This period straddles the diatom record at the top of YC2

617 (zone YC2-IV) and the bottom of YC1 (zone YC1-I). The diatom assemblage is notable for
618 its dominance by *N. (C.) elkab* and *N. (C.) halophila* (both cores), with *Nitzschia frustulum*
619 and *N. palea* (Fig. 6). The switch to an *N. elkab/N. halophila* flora is consistent with a
620 return to more alkaline conditions, probably driven by increasing evaporation. *Navicula*
621 (*C.*) *elkab* does seem to have a distinct ecology, with a preference for hyper-alkaline,
622 Na₂CO₃ lakes, where Cl⁻ is also important. *Nitzschia frustulum* tends to be more abundant
623 with *N. (C.) elkab* than with *N. (C.) halophila* (e.g. YC2-4c and base of YC1-1) supporting
624 the interpretation of high alkalinity (Gasse, 1986). Its presence with *N. palea* again seems
625 to indicate high levels of nutrient enrichment. Overall, this assemblage is quite similar to
626 that sampled from the modern lake in 1982, when it was around 2 metres deep. A peak
627 in magnetic susceptibility between about 5,500 and 4,500 BP (Fig. 3) associated with a
628 sharp reduction in $\delta^{18}\text{O}_{\text{carb}}$ (Fig. 4) points to a climatically-controlled inwash event, which
629 may be reflected by rather poor diatom preservation in YC1.

630

631 After 4,500 aBP, $\delta^{18}\text{O}_{\text{carb}}$ remained high although with some short-lived negative
632 excursions, whereas $\delta^{13}\text{C}_{\text{carb}}$ values are reduced dramatically (Fig. 4). For the interval of
633 overlap between YC1 and YC2, there is good agreement between the isotope records,
634 especially so for $\delta^{13}\text{C}_{\text{carb}}$, once allowance is made for the slight age difference between the
635 two cores, as discussed earlier. There is a large increase in ostracod concentration within
636 much of this interval: the dominance of assemblages by *L. sappaensis*, coupled with the
637 large number of individuals, is consistent with the lake having been saline and alkaline for
638 much of the time (Fig. 4). $\delta^{18}\text{O}_{\text{ostracod}}$ values are ¹⁸O-enriched compared to $\delta^{18}\text{O}_{\text{carb}}$ values,
639 with the degree of enrichment consistent with vital offsets from oxygen-isotope equilibrium,
640 as discussed above. The $\delta^{13}\text{C}_{\text{ostracod}}$ values agree well with those for $\delta^{13}\text{C}_{\text{carb}}$, suggesting
641 that the two sources of carbonate formed under the same set of conditions, as was the
642 case for the interval prior to the positive $\delta^{13}\text{C}_{\text{carb}}$ excursion. The diatom record for this

643 interval was published by Metcalfe and Hales (1994), although here we plot the data
644 against our new age model (Fig. 6). The species encountered confirm the presence of a
645 shallow alkaline lake throughout the late Holocene, although the balance between CO_3^{2-}
646 and Cl^- seems to have varied. The assemblage in zone YC1-II, for example, may indicate
647 that Cl^- replaced CO_3^{2-} as the dominant anion. The assemblage is similar to Bradbury's
648 (1989) saline marsh group. Fresher conditions were then re-established, associated with
649 inwash from the catchment. This wetter/drier cycle is then repeated in zones YC1-III and
650 YC1-IV. Increasingly hostile conditions for diatom preservation are indicated through zone
651 YC1-V, with only a patchy diatom record between about 2000 and 1200 aBP. It seems
652 likely that the single count available through this period is significantly affected by
653 differential preservation. The diatom record resumes around 1000 aBP with a distinctive,
654 well-preserved sample dominated (55%) by *Navicula muralis* (zone YC1-VII). This diatom
655 is often found on mud flats and amongst aquatic vegetation (Hustedt, 1961-66). When
656 combined with very low magnetic susceptibility values, the diatom assemblages indicate
657 catchment stability. We note that this catchment stability occurs at a time in the late
658 Classic when many sites in the relatively dry parts of Central Mexico were abandoned
659 (Beekman, 2010; Park *et al.*, 2010). The most recent sediments preserve a flora quite
660 similar to that found in the various surface sediment samples, indicating a shallow alkaline
661 lake, but with increasing nutrient levels. The very highly evolved chemistry and rather
662 distinctive diatom flora of La Piscina de Yuriria is described in Davies *et al.* (2002) and
663 sampling in 2003 and 2004 confirmed its hypereutrophic status. Phases of inwash,
664 previously reported in YC1 and attributed to anthropogenic disturbance (Metcalfe *et al.*,
665 1994), are also seen at broadly the same times in YC2, i.e. around 3,600 and 1500 aBP
666 and over the past few centuries. An earlier phase at the base of YC1, which ended in that
667 core around 4700 aBP, appears in its entirety in YC2, starting around 5600 aBP. The
668 absence of *Z. mays* pollen from YC1 during this interval led Metcalfe *et al.* (1994) to

669 suggest that the inwash was climatically-mediated rather than the result of anthropogenic
670 disturbance. For the wider region however, Park *et al.* (2010) suggest that agricultural
671 activity began as early as around 5700 aBP (based on the presence of *Zea* pollen), and
672 expanded around 3000 aBP. Lozano *et al.* (2013) also report the occurrence of *Z. mays*
673 pollen from 3000 aBP in Lake Zirahuén, a lake previously thought to be un-affected by
674 human impact. The main climatic and environmental changes revealed in the records from
675 La Piscina de Yuriria are summarised in Table 2.

676

677 There is a reasonable correspondence between phases of inwash, as indicated by
678 magnetic susceptibility and 'inwash' elements, and intervals of low ostracod abundance for
679 the whole of the Holocene (Fig. 7). This suggests that increased turbidity in the lake, which
680 would likely have arisen during phases of increased inwash, was unfavourable for
681 ostracod survival as has been noted previously (e.g. Bridgwater *et al.*, 1999). Therefore
682 water turbidity is an additional control to hydrochemistry on ostracod assemblages in La
683 Piscina de Yuriria.

684

685 The number of palaeoclimatic records from the TMVB (and indeed the whole of Mexico),
686 extending back to 30,000 BP (Marine Isotope Stage 3) is small and limited to the Basin of
687 Mexico (e.g. Caballero and Ortega-Guerrero, 1998; Roy *et al.*, 2009; Lozano-García *et al.*,
688 2015), Lake Cuitzeo (Israde *et al.*, 2010), Lake Pátzcuaro (Watts and Bradbury, 1982;
689 Bradbury 2000) and Lake Zacapu (Correa-Metrio *et al.*, 2012). Moreover, most of these
690 have limited dating control for the older sediments. Caballero *et al.* (2010) integrated
691 palaeolimnological records with evidence from glacial chronologies (Vazquez Selem and
692 Heine, 2004) to provide a palaeoclimatic scenario for the period from around 30,000 aBP
693 to the last glacial maximum (LGM). A more recent consideration of the record from Lake
694 Chalco in the Basin of Mexico has been published by Lozano-García *et al.* (2015). With

695 the exception of Lake Pátzcuaro (one of the westernmost sites), the records suggest
696 drying and cooling after about 30,000 aBP, with glacial advances restricted until around
697 22,000 aBP. The data from La Piscina de Yuriria suggest that there were rapid shifts
698 between wet and dry conditions during this interval, with a general drying trend sometime
699 between about 27,500 and 25,000 aBP. However, the relatively low resolution of the
700 record after about 27,500 aBP means that a continuation of abrupt shifts in rainfall cannot
701 be ruled out. Major glacial advances in the TMVB occurred around the LGM (22,000 –
702 18,000 aBP) with a suggested 6 – 8°C lowering in mean annual temperature. Reduced
703 temperature, along with low effective moisture, could have contributed to the elevated
704 $\delta^{18}\text{O}_{\text{carb}}$ values at this time. Although generally dry, there seem to have been short lived
705 lake highstands in Cuitzeo and rising water levels in the Chalco Basin (southern Basin of
706 Mexico) and the Lerma Basin around 18,000 and 19,000 aBP respectively (Caballero *et*
707 *al.*, 2002). Unfortunately the evidence from La Piscina de Yuriria is at too low resolution to
708 be able to detect these highstands. The late glacial in the TMVB (18,000 – 15,000 aBP) is
709 described as cold and dry, with minor glacial recession (Caballero *et al.*, 2010): evidence
710 from La Piscina de Yuriria indicates a continuation of dry conditions through the late glacial
711 (=Younger Dryas) stadial. Significant warming and glacial retreat apparently started
712 around 14,000 aBP.

713

714 Overall, the records of cool and dry conditions around the LGM and into the early
715 Holocene from the central and eastern part of the TMVB are most easily explained by a
716 reduction in summer season precipitation, which is driven today by the northward
717 movement of the ITCZ and the onset of the NAM. Records from the Pátzcuaro Basin, to
718 the west of this group, show high lake levels persisting through the LGM (Bradbury 2000;
719 Metcalfe *et al.*, 2007), while Correa-Metrio *et al.* (2012) suggest conditions moist enough
720 for pine forest to dominate over grasslands in the Zacapu basin. In both cases an increase

721 in winter precipitation may provide an explanation although it is hard to reconcile this with
722 the stable-isotope data from La Piscina de Yuriria, which suggest an overall decrease in
723 effective moisture. Lachniet *et al.* (2013) have further suggested that the summer
724 monsoon did not collapse during the last glacial, although once again the evidence from
725 La Piscina de Yuriria does not appear to support this, nor does the latest interpretation of
726 the Chalco record (Lozano-Garcia *et al.*, 2015). The late glacial stadial was a time of dry
727 conditions, with some suggestion that La Piscina de Yuriria may have dried out. A dry
728 Younger Dryas stadial has also been reported from Zacapu (Correa-Metrio *et al.*, 2012)
729 and from sites in northern Mexico (e.g. Roy *et al.*, 2013). Interestingly, the Younger Dryas
730 is also reported as dry in the Juxtlahuaca speleothem record (Lachniet *et al.*, 2013) where
731 it is attributed to monsoon collapse. It appears that the weakening of the Atlantic
732 Meridional circulation (AMOC), the subsequent southward displacement of the ITCZ and a
733 weaker monsoon led to dry conditions over the northern hemisphere neotropics (Bush and
734 Metcalfe, 2012). Only at the northern edge of the NAM region did the resumption of cold
735 conditions allow more penetration of mid-latitude westerlies leading to wetter conditions
736 (Metcalfe *et al.*, 2015).

737

738 The classic pattern of climatic change in the NH tropics and subtropics is for wetter
739 conditions in the early Holocene driven by poleward migration of the ITCZ and a stronger
740 monsoon in response to insolation forcing. Whilst there is some support from this in
741 Mexico, it seems that the establishment of the modern climatic regime was delayed by the
742 presence of the residual Laurentide Ice Sheet and the influence of meltwater pulses
743 entering the Gulf of Mexico (Metcalfe *et al.*, 2015). The early Holocene interval in La
744 Piscina de Yuriria indicates a change to wetter conditions overall, but with evidence for
745 abrupt shifts between wet and dry conditions. A similar pattern is recorded by Park *et al.*
746 (2010) for their other sites in the Valle de Santiago. The response of the wider NAM region

747 to the insolation maximum in the early Holocene is complex, with the clearest response in
748 the south, where the direct influence of the ITCZ is strongest. Elsewhere, it seems that the
749 modern NAM regime may not have resumed until after 8000 aBP and there was a trade-
750 off between increasing precipitation and increasing temperatures (Metcalf *et al.*, 2015).
751 La Piscina de Yuriria shows an overall trend of drying from the mid Holocene onwards.
752 This is consistent with the southward migration of the ITCZ and as the role of insolation
753 forcing became weaker, so the effect of other climate forcings such as ENSO, seems to
754 have become more important giving rise to increasingly complex patterns of change. This
755 drying was accompanied by increasing human impact, as shown by evidence for phases
756 of sediment inwash and by the presence of *Z. mays* pollen. Increasing human impact
757 during this interval is also evident from other sites in Mexico (Metcalf *et al.*, 1994).

758

759 **Conclusions**

760 In summary, evidence from La Piscina de Yuriria indicates that the climate of Central
761 Mexican highlands has changed dramatically over the past ~30,000 years. Between
762 30,000 and about 27,500 aBP it was highly variable with shifts, which may have been
763 abrupt, between dry and wet conditions. Over much of the glacial period, from ~27,500 to
764 about 14,000 aBP, climate became drier: there may have been abrupt shifts during this
765 interval, but the low resolution of our data means that any such shifts are not revealed.
766 The occurrence of strong millennial scale variability during MIS3, with a global signature,
767 has been widely noted (Clement and Peterson, 2008), apparently driven by changes in
768 AMOC. It is notable that there were three D/O warming events (2 – 4) between 30,000 and
769 22,000 aBP (Wolff *et al.*, 2010) and two Heinrich events (H2 and H3). Modelling has
770 indicated differential sensitivity of AMOC under MIS3 and LGM conditions (e.g. Van
771 Meerbeeck *et al.* 2009), with the climate becoming less sensitive to AMOC changes as the
772 full glacial climate was established. The growth of the Laurentide Ice sheet from an

773 interstadial minimum around 35,000 aBP to its maximum by ca. 25,000 aBP (where it
774 remained until around 15,000 aBP) (Dyke et al., 2002) also reflects the shift of the global
775 climate system into full glacial mode, where other, less rapid forcings may have dominated
776 (see Baker and Fritz, 2015). There is evidence of drought during the period that
777 encompassed the late glacial stadial. During the Holocene, the climate initially became
778 wetter, although the positive water balance was insufficient to lead to major changes in the
779 lake's chemistry and diatom flora. A fall in lake levels under drier climate in the mid
780 Holocene was accompanied by a change in limnology that caused methane formation.
781 Inwash of catchment soils and sediments was the result of a combination of natural
782 climatic triggers and, for the later Holocene, anthropogenic disturbance.

783

784 *Acknowledgements*

785 SEM and HLJ would like to acknowledge Professor Alayne Street-Perrott for introducing
786 them to Mexico and its many and varied lakes, including La Piscina de Yuriria. She led
787 the Tropical Palaeoenvironments Research Group that took both the cores presented here
788 and supervised the early work on these. We also acknowledge the pivotal role that the
789 late Alan Perrott played in recovering lake-sediment cores from Mexico. Some of this work
790 was funded by a University studentship from Kingston University to HLJ. We acknowledge
791 support from NERC (radiocarbon dating allocation 549/0993 and stable isotope allocations
792 IP/334/0992). Some of the sedimentological and geochemical analyses on core YC2 were
793 undertaken by Nick Barber, formerly of University of Oxford. We thank Tim Heaton, NERC
794 Isotope Geosciences Laboratory, for isotope analyses of waters and ostracod shells. The
795 geochemical results from YC1 were part of Philip Hales' DPhil thesis (supervised by AS-
796 P). SEM would like to acknowledge the work of her former student, Laura Park, for
797 undertaking the initial diatom counts on YC2.

798

799

800 **References**

801 Aharon P. 2003. Meltwater flooding events in the Gulf of Mexico revisited: implications for
802 rapid climate changes during the last deglaciation. *Paleoceanography*, **18**: 1079,
803 doi:10.1029/2002PA000840

804

805 Alcocer J, Escobar E, Lugo A. 2000. Water use (and abuse) and its effects on the crater-
806 lakes of Valle de Santiago, Mexico. *Lakes & Reservoirs: Research & Management*,
807 **5**: 145–149.

808

809 Aranda-Gómez JJ, Levresse G, *et al.* 2013, Active sinking at the bottom of the Rincón de
810 Parangueo Maar (Guanajuato, México) and its probable relation with subsidence faults at
811 Salamanca and Celaya. *Boletín de la Sociedad Geológica Mexicana*, **65**: 169-188.

812

813 Baker PA, Fritz SC. 2015. Nature and causes of Quaternary climate variation of tropical
814 South America. *Quaternary Science Reviews*, **124**: 31-47.

815

816 Barker P, Fontes J-C, Gasse F, Druart JC. 1994. Experimental dissolution of diatom silica
817 in concentrated salt solutions and implications for palaeoenvironmental reconstruction.
818 *Limnology and Oceanography*, **39**: 99-110.

819

820 Battarbee, R.W. 1986. Diatom Analysis. In: *Handbook of Holocene Palaeoecology and*
821 *Palaeohydrology* [Berglund BE, (Ed.)] John Wiley & Sons Ltd: New York; pp. 527-570.

822

823 Beekman CS. 2010. Recent research in Western Mexican archaeology. *Journal of*
824 *Archaeological Research* **18**: 41-109.

825

826 Bernal JP, Lachniet M, McCulloch M, Mortimer G, Morales P, Cienfuegos E. 2011. A
827 speleothem record of Holocene climate variability from southwestern Mexico. *Quaternary*
828 *Research*, **75**: 104-113

829

830 Blaauw M. 2010. Methods and code for 'classical' age-modelling of radiocarbon
831 sequences. *Quaternary Geochronology*, **5**: 512-518.

832

833 Bradbury JP. 1989. Late Quaternary lacustrine paleoenvironments in the Cuenca de
834 Mexico. *Quaternary Science Reviews*, **8**: 75-100.

835

836 Bradbury JP. 2000 Limnologic history of Lago de Pátzcuaro, Michoacán, Mexico for the
837 past 48,000 years: impacts of climate and man. *Palaeogeography Palaeoclimatology*
838 *Palaeoecology* **63**: 169-195.

839

840 Bridgwater ND, Heaton THE, O'Hara SL. 1999. A late Holocene palaeolimnological record
841 from central Mexico, based on faunal and stable-isotope analysis of ostracod shells.
842 *Journal of Paleolimnology*, **22**: 383-397.

843

844 Brown RB. 1985. A summary of Late-Quaternary pollen records from Mexico west of the
845 Isthmus of Tehuantepec. In: *Pollen Records of Late Quaternary North American*
846 *Sediments*. [Bryant VM, Holloway RG. (Eds.)]. American Association of Stratigraphic
847 Palynologists: Dallas; pp. 71-92.

848

849 Bush MB, Metcalfe SE, 2012 Latin America and the Caribbean. In: *Quaternary*
850 *Environmental Change in the Tropics*. [Metcalfe SE, Nash DJ. (Eds)]. J. Wiley & Sons:
851 Chichester; pp. 263-311.

852

853 Butzer K, Butzer, EK. 1993. The sixteenth-century environment of the Central Bajío:
854 Archival reconstruction from Colonial land grants and the question of Spanish ecological
855 impact In: *Culture, Form and Place*. [Mathewson K. (Ed.)] Baton Rouge, LA, *Geoscience*
856 *and Man* **32**: pp. 89-124.

857

858 Caballero M, Ortega-Guerrero B. 1998. Lake levels since 40,000 years ago at Chalco
859 Lake, near Mexico City. *Quaternary Research*, **50**: 90-106.

860

861 Caballero, M, Ortega, B, Valadéz, F, Metcalfe, S, Macías, J, Sugiura, Y. 2002. Sta. Cruz
862 Atizapan: a 22-ka lake level record and climatic implications for the late Holocene human
863 occupation in the upper Lerma Basin. *Palaeogeography, Palaeoclimatology,*
864 *Palaeoecology*, **186**: 217-235.

865

866 Caballero M, Lozano-García S, Vázquez-Selem L, Ortega B. 2010. Evidencias de cambio
867 climático y ambiental en registros glaciales y en cuencas lacustres del centro de México
868 durante el último máximo glacial. *Boletín de la Sociedad Geológica Mexicana*, **62**: 359-
869 377.

870

871 Clement AC, Peterson LC. 2008. Mechanisms of abrupt climate change of the last glacial
872 period. *Reviews of Geophysics*, **46**, RG4002/2008.

873

874 Cohen AS. 2003. *Paleolimnology: the history and evolution of lake systems*. Oxford
875 University Press: New York; 528 pp.
876
877 Correa-Metrio A, Lozano-Garcia S, Xelhuantzi-Lopez S, Sosa-Najera S, Metcalfe SE.
878 2012. Vegetation in western Central Mexico during the last 50,000 years: modern analogs
879 and climate in the Zacapu Basin. *Journal of Quaternary Science*, **27**: 509-518.
880
881 Davies HL. 1995. *Quaternary Palaeolimnology of a Mexican Crater Lake*. Unpublished
882 PhD thesis, Kingston University.
883
884 Davies SJ. 2000. *Environmental change in the west-central Mexican highlands over the*
885 *last 1,000 years: evidence from lake sediments*. Unpublished PhD thesis, University of
886 Edinburgh.
887
888 Davies, SJ, Metcalfe, SE, Caballero, ME, Juggins, S. 2002. Developing diatom-based
889 transfer functions for Central Mexican lakes. *Hydrobiologia*, **467**: 199-213.
890
891 De Deckker P, Forester RM. 1988. The use of ostracods to reconstruct
892 palaeoenvironmental records. In: *Ostracods in the Earth Sciences*. [De Deckker P, Colin J-
893 P, Peypouquet, J-P. (Eds.)] Elsevier: Amsterdam; pp.175-199.
894
895 Dean, W.E. 1974. Determination of carbonate and organic matter in calcareous sediments
896 and sedimentary rocks by loss of ignition: comparison with other methods. *Journal of*
897 *Sedimentary Petrology*. **44**: 242-248.
898

899 Dean WE, Gorham E. 1976. Major chemical and mineral components of profundal surface
900 sediments in Minnesota lakes. *Limnology and Oceanography*, **21**: 259-284.
901

902 Decrouy L, Vennemann TW, Ariztegui D. 2011. Controls on ostracod valve geochemistry,
903 Part 1: variations of environmental parameters in ostracod (micro-) habitats. *Geochimica et*
904 *Cosmochimica Acta*, **75**: 7364–7379.

905 Dyke AS, Andrews JT, Clark PU, England JH, Miller GH, Shaw J, Veillette JJ. 2002. The
906 Laurentide and Innuitian ice sheets during the Last Glacial Maximum. *Quaternary Science*
907 *Reviews* **21**: 9-31.
908

909 Engstrom DR, Wright HEJ. 1984. Chemical stratigraphy of lake sediments as a record of
910 environmental change. In: *Lake Sediments and Environmental History*. [Haworth Y, Lund
911 E. (Eds.)]. Leicester University Press: Leicester; pp. 11-67.
912

913 Eugster HP, Hardie LA. 1978. Saline Lakes. In: *Lakes: Chemistry, Geology, Physics*.
914 [Lerman A. (Ed.)]. Springer-Verlag: New York; pp. 237–294.
915

916 Forester RM. 1986. Determination of the dissolved anion composition of ancient lakes
917 from fossil ostracodes. *Geology*, **14**: 796-798.
918

919 Gasse, F., 1986. East African Diatoms. Taxonomy, ecological distribution. *Bibliotheca*
920 *Diatomologica*. **11**: J. Cramer: Stuttgart; 202 pp.
921

922 Gasse F, Barker P, Gell PA, Fritz SC, Chalié, F. 1997. Diatom-inferred salinity in
923 palaeolakes: an indirect tracer of climate change. *Quaternary Science Reviews*, **16**: 547-
924 563.

925

926 Goldsmith JR, Graf DL, and Heard HC. 1961. Lattice Constants of the Calcium-
927 Magnesium Carbonates. *American Mineralogist*, **43**: 84-101.

928

929 Goman M, Byrne R. 1998. A 5000-year record of agriculture and tropical forest clearance
930 in the Tuxtlas, Veracruz, Mexico. *The Holocene* **8**: 83-89.

931

932 Gomez de Orozco, F. 1972. *Cronícas de Michoacán*. UNAM: Mexico; 214 pp.

933

934 Gorenstein S, Pollard HP. 1983. The Tarascan civilisation: a late Prehispanic cultural
935 system. *Publications in Anthropology* **28**: Vanderbilt University Press, Nashville,
936 Tennessee. 199 pp.

937

938 Grimm EC. 1987. CONISS: a FORTRAN 77 program for stratigraphically constrained
939 cluster analysis by the method of incremental sum of squares. *Computers and*
940 *Geoscience*, **13**: 13-35

941

942 Gu B, Schelske CL, Hodell DA. 2004. Extreme ¹³C enrichment in a shallow hypereutrophic
943 lake: implications for carbon cycling. *Limnology and Oceanography*, **49**: 1152–1159.

944

945 Hill MO. 1979. TWINSPAN: A FORTRAN program for arranging multivariate data in an
946 ordered two-way table by classification of the individuals and attributes. *Ecology and*
947 *Systematics*, Cornell University: New York; 48 pp.

948

949 Hill E. 2006. *Quantitative reconstruction of eutrophication histories in Central Mexican*
950 *lakes*. Unpublished PhD thesis, University of Nottingham.

951

952 Hustedt, F., 1961-1966. *Die Kieselalgen Deutschlands, Österreichs und der Schweiz*, Vol.
953 **3**. Reprinted 1977, Otto Koeltz: Koenigstein; 816 pp.

954

955 Israde Alcántara I, Velázquez-Duran R, Lozano García MS, Bischoff J, Dominquez
956 Vázquez G, Garduño Monroy VH. 2010. Evolución paleolimnológica del Lago Cuitzeo,
957 Michoacán durante el Pleistoceno-Holoceno. *Boletín de la Sociedad Geológica*
958 *Mexicana*, **62**: 345-357.

959

960 Jongman RHG, ter Braak CJF, Van Tongeren OFR (Eds.) 1992. *Data Analysis in*
961 *Community Ecology and Landscape Ecology*. Cambridge University Press: Cambridge;
962 324 pp.

963

964 Kienel U, Wulf Bowen S, Byrne R, Park J, Bohnel H, Dulski P, Luhr JF, Siebert L, Haug
965 GH, Negendank JFW, 2009. First lacustrine varve chronologies from Mexico: impact of
966 droughts, ENSO and human activity since AD 1840 as recorded in maar sediments from
967 Valle de Santiago. *Journal of Paleolimnology*, **42**: 587-609.

968

969 Kilham P, Kilham SS, Hecky RE. 1986. Hypothesized resource relationships among
970 African planktonic diatoms. *Limnology and Oceanography*, **31**: 1169-1181.

971

972 Krammer K. Lange-Bertalot H. 1988. *Süßwasserflora von Mitteleuropa*.
973 *Bacillariophyceae. 2. Teil: Epithemiaceae, Bacillariaceae, Surirellaceae*. Vol. 2/2. Gustav
974 Fischer Verlag: Stuttgart; 596 pp.

975

976 Krammer K. Lange-Bertalot H. 1991a. *Süsswasserflora von Mitteleuropa*.
977 *Bacillariophyceae. 3. Teil: Centrales; Fragilariaceae, Eunotiaceae*. Vol. 2/3. Gustav
978 Fischer Verlag: Stuttgart; 576 pp.
979
980 Krammer K. Lange-Bertalot H. 1991b. *Süsswasserflora von Mitteleuropa*.
981 *Bacillariophyceae. 4. Teil: Achnantheaceae*. Vol. 2/4. Gustav Fischer Verlag: Stuttgart; 437
982 pp.
983
984 Lachniet MS, Asmerom Y, Bernal JP, Polyak VJ, Vazquez-Selem L. 2013. Orbital pacing
985 and ocean circulation-induced collapses of the Mesoamerican monsoon over the past
986 22,000 y. *Proceedings of the National Academy of Sciences*, **110**: 9255-9260.
987
988 Lamb AL, Leng MJ, Lamb HF, Ummer M. 2000. A 9000-year oxygen and carbon isotope
989 record of hydrological change in a small Ethiopian crater lake. *The Holocene*, **10**: 167-177.
990
991 Lozano-García S, Vázquez-Selem L. 2005. A high-elevation Holocene pollen record from
992 Iztaccíhuatl volcano, central Mexico. *The Holocene*, **15**: 329-338.
993
994 Lozano-García, S., Sosa-Nájera, S., Sugiura, Y. and Caballero, M. 2005. 23,000 yr of
995 vegetation history of the Upper Lerma, a tropical high-altitude basin in Central Mexico.
996 *Quaternary Research* 64, 70-82.
997
998 Lozano-García S, Torres-Rodríguez E, Ortega B, Vázquez G, Caballero M. 2013.
999 Ecosystem responses to climate and disturbances in western central Mexico during the
1000 late Pleistocene and Holocene. *Palaeogeography Palaeoclimatology Palaeoecology*,
1001 **370**: 184-195.

1002

1003 Lozano-Garcia S, Ortega B., Roy P, Beramendi-Orosco L, Caballero, M. 2015. Climatic
1004 variability in the northern sector of the American tropics since the latest MIS3. *Quaternary*
1005 *Research*, **84**: 262-271.

1006

1007 Martens K. 1994. Summary of the morphology, taxonomy and distribution of *Limnocythere*
1008 *inopinata* (Baird, 1843) (Ostracoda, Limnocytheridae). In; *The evolutionary ecology of*
1009 *reproductive modes in non-marine Ostracoda*. [Horne DJ, Martens K. (Eds.)]. The
1010 University of Greenwich Press: Greenwich; pp. 17-22.

1011

1012 Metcalfe SE. 1990. *Navicula elkab* O. Müller – a species in need of redefinition? *Diatom*
1013 *Research*, **5**: 419-423.

1014

1015 Metcalfe SE, Street-Perrott FA, Brown RB, Hales PE, Perrott RA, Steininger FM. 1989.
1016 Late Holocene Human Impact on Lake Basins in Central Mexico. *Geoarchaeology*, **4**: 119-
1017 141.

1018

1019 Metcalfe SE, Hales PE. 1994. Holocene Diatoms From A Mexican Crater Lake : La
1020 Piscina De Yuriria. *Memoirs of the California Academy of Sciences*, **17**: 501-515.

1021

1022 Metcalfe SE, Street-Perrott FA, O'Hara SL, Hales PE, Perrott RA (1994) The
1023 palaeolimnological record of environmental change: examples from the arid frontier of
1024 Mesoamerica. In: *Environmental Change in Drylands: Biogeographical and*
1025 *Geomorphological Perspectives*. [Millington AC, Pye K. (eds.)]. John Wiley and Sons Ltd:
1026 Chichester; pp.131-145

1027

1028 Metcalfe SE, Davies SJ, Braisby JD, Leng MJ, Newton AJ, Terrett NL, O'Hara SL. 2007.
1029 Long and short-term change in the Patzcuaro Basin, central Mexico. *Palaeogeography*
1030 *Palaeoclimatology Palaeoecology*, **247**: 272-295.

1031

1032 Metcalfe SE, Barron JA, Davies SJ. 2015. The Holocene history of the North American
1033 Monsoon: 'known knowns' and 'known unknowns' in understanding its spatial and
1034 temporal complexity. *Quaternary Science Reviews*, **120**: 1-27.

1035

1036 Ordoñez E. 1900. Les volcans du Valle de Santiago. *Memorias de la Sociedad Científica*
1037 *Antonio Alzate (Mexico)* **14**: 299-326.

1038

1039 Park LA. 1999. *Late Quaternary environmental change in La Piscina de Yuriria, Central*
1040 *Mexico: evidence from the palaeolimnological record*. Unpublished MRes thesis,
1041 University of Edinburgh.

1042

1043 Park J, Byrne R, Bohnel H, Molina Garza R, Conserva M. 2010. Holocene climate change
1044 and human impact, central Mexico: a record based on maar lake pollen and sediment
1045 chemistry. *Quaternary Science Reviews*, **29**: 618-632.

1046

1047 Patrick R. Reimer C.W. 1966. The diatoms of the United States exclusive of Alaska and
1048 Hawaii. Vol. 1. *The Academy of Natural Sciences of Philadelphia, Philadelphia,*
1049 *Monograph*, **13**: 668 pp.

1050

1051 Patrick, R. & C. W. Reimer, 1975. The diatoms of the United States exclusive of Alaska
1052 and Hawaii. Vol. 2. Part 1. *The Academy of Natural Sciences of Philadelphia, Philadelphia,*
1053 *Monograph*, **13**: 213 pp.

1054

1055 Reimer PJ, Bard E, Bayliss A, Beck JW, Blackwell PG, Ramsey CB, Buck CE, Cheng H,
1056 Edwards RL, Friedrich M, Grootes PM, Guilderson TP, Hafliðason H, Hajdas I, Hatte,
1057 C, Heaton TJ, Hoffmann DL, Hogg AG, Hughen KA, Kaiser KF, Kromer B, Manning SW,
1058 Niu M, Reimer RW, Richards DA, Scott EM, Southon JR, Staff RA, Turney CSM, van der
1059 Plicht J. 2013. Intcal13 and Marine13 Radiocarbon Age Calibration Curves 0-50,000 Years
1060 Cal BP. *Radiocarbon*, **55**: 1869-1887.

1061

1062 Roy PD, Caballero M, Lozano R, Pi T, Morton O. 2009. Late Pleistocene-Holocene
1063 geochemical history inferred from Lake Tecocomulco sediments, Basin of Mexico, Mexico.
1064 *Geochemical Journal*, **43**: 49-64.

1065

1066 Roy PD, Quiroz-Jimenez JD, Perez-Cruz L, Lozano-Garcia S, Metcalfe SE, Lozano-
1067 Santacruz R, Lopez-Balbiaux N, Sanchez-Zavala JL, Romero FM. 2013. Late Quaternary
1068 paleohydrological conditions in the drylands of northern Mexico: a summer precipitation
1069 proxy record of the last 80 cal ka BP. *Quaternary Science Reviews*, **78**: 342-354.

1070

1071 Schoeman FR, Archibald REM. 1977. *The Diatom Flora of South Africa*, Nos. 1-6. CSIR
1072 Special Report WAT 50. Pretoria.

1073

1074 Sears PB, Clisby K. 1955. Palynology in southern North America, Part IV: Pleistocene
1075 climate in Mexico. *Bulletin of the Geological Society of America*, **66**: 521-530.

1076

1077 Talbot MR. 1990. A review of the palaeohydrological interpretation of carbon and oxygen
1078 isotope ratios in primary lacustrine carbonates. *Chemical Geology (Isotope Geosciences*
1079 *Section)*, **80**: 261-279.

1080

1081 Tarutani T, Clayton RN, Mayeda TK 1969. The effect of polymorphism and magnesium
1082 substitution on oxygen isotope fractionation between calcium carbonate and water.
1083 *Geochimica et Cosmochimica Acta*, 33, 987–996.

1084

1085 ter Braak CJF. 1988a. CANOCO - a FORTRAN program for canonical community
1086 ordination by [partial] [detrended] [canonical] correspondence analysis, principal
1087 components analysis and redundancy analysis (version 2.1). Report LWA-88-02.
1088 Agricultural Mathematics Group: Wageningen.

1089

1090 Van Meerbeeck CJ, Renssen H, Roche DM. 2009. How did Marine Isotope Stage 3 and
1091 Last Glacial Maximum climates differ? – perspectives from equilibrium simulations.
1092 *Climate of the Past*, 5: 33-51.

1093

1094 Vazquez-Selem L, Heine, K. 2004 Late Quaternary glaciation in Mexico. In: *Quaternary*
1095 *Glaciations – Extent and Chronology. Part III South America, Asia, Africa, Australia,*
1096 *Antarctica*. [Ehlers J, Gibbard P. (Eds.)] Elsevier: Amsterdam; pp. 233-242.

1097

1098 von Grafenstein U, Erlenkeuser H, Trimborn P. 1999. Oxygen and carbon isotopes in
1099 modern fresh-water ostracod valves: assessing vital offsets and autecological effects of
1100 interest for palaeoclimate studies. *Palaeogeography Palaeoclimatology Palaeoecology*,
1101 **148**: 133-152.

1102

1103 Watts WA, Bradbury JP 1982. Late Pleistocene and Holocene paleoenvironments and
1104 human activity in the West-Central Mexican Plateau - evidence from Lake Pátzcuaro,
1105 Michoacán, and from the Cuenca de Mexico. *Quaternary Research*, 17: 56-70.

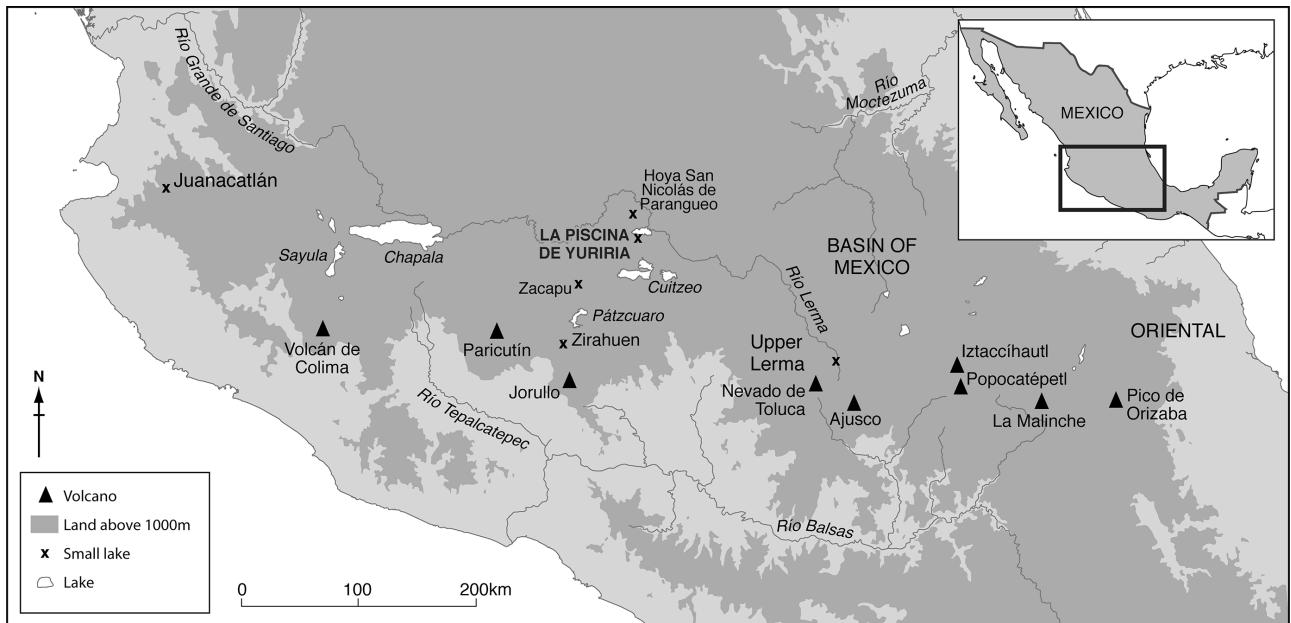
1106

1107 Wolff EW, Chappellaz J, Blunier T, Rasmussen SO, Svensson A. 2010. Millennial-scale
1108 variability during the last glacial: the ice core record. *Quaternary Science Reviews*, **29**:
1109 2828-2838.

1110

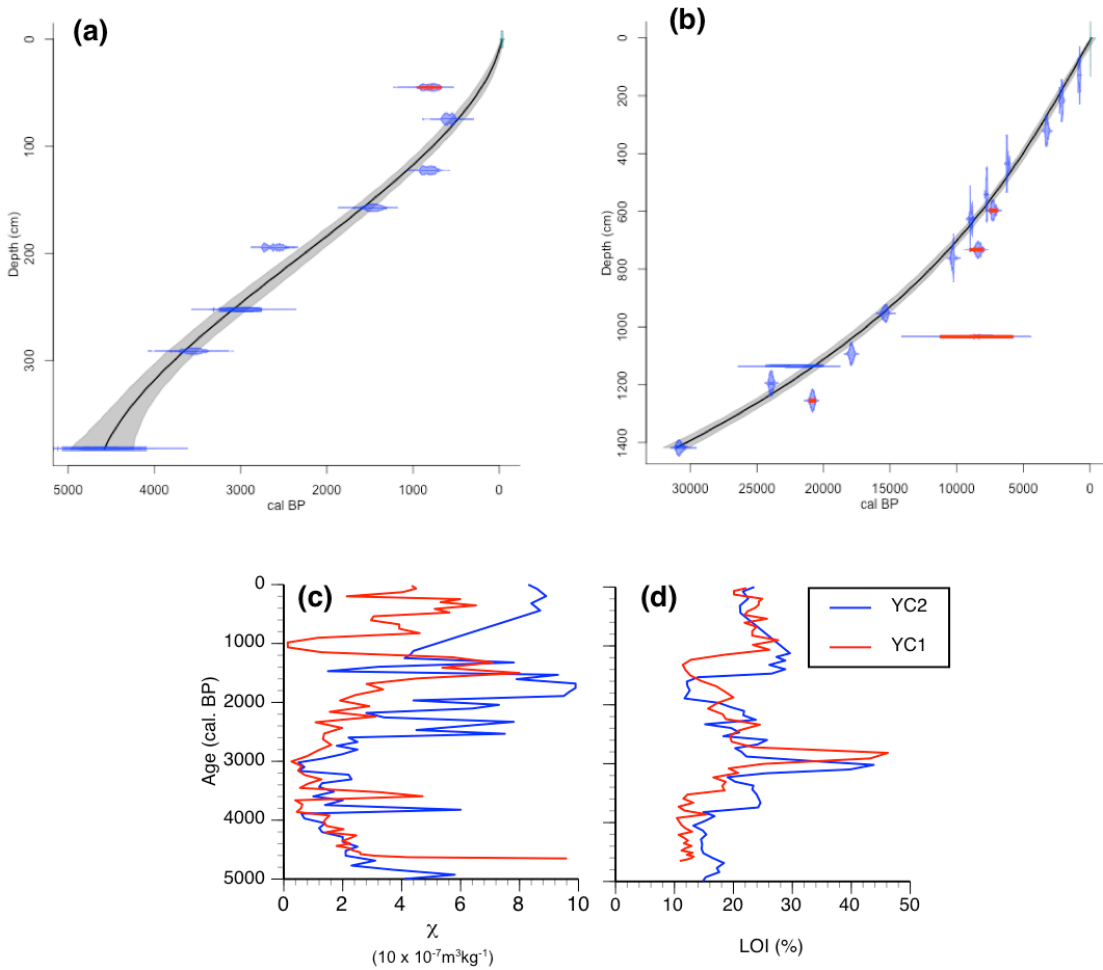
1111

1112 **Figures**



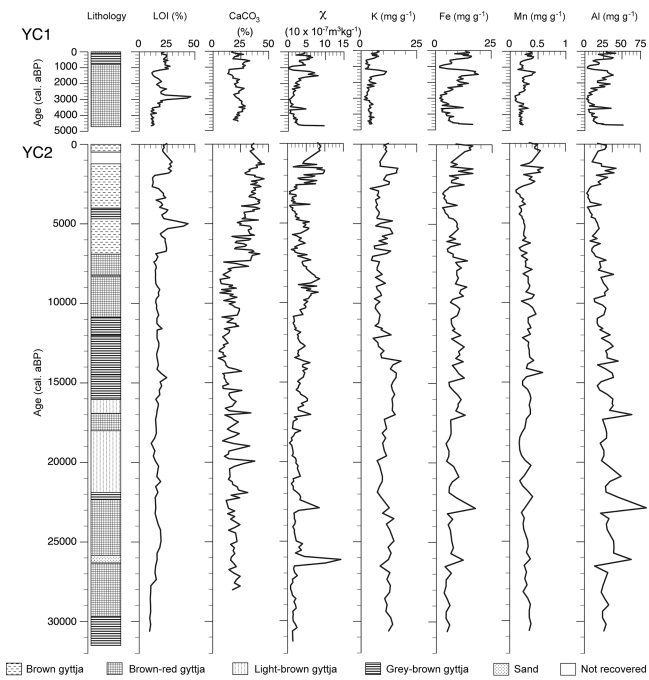
1113

1114 Fig. 1. Location of la Piscina de Yuriria and other sites referred to in the text.



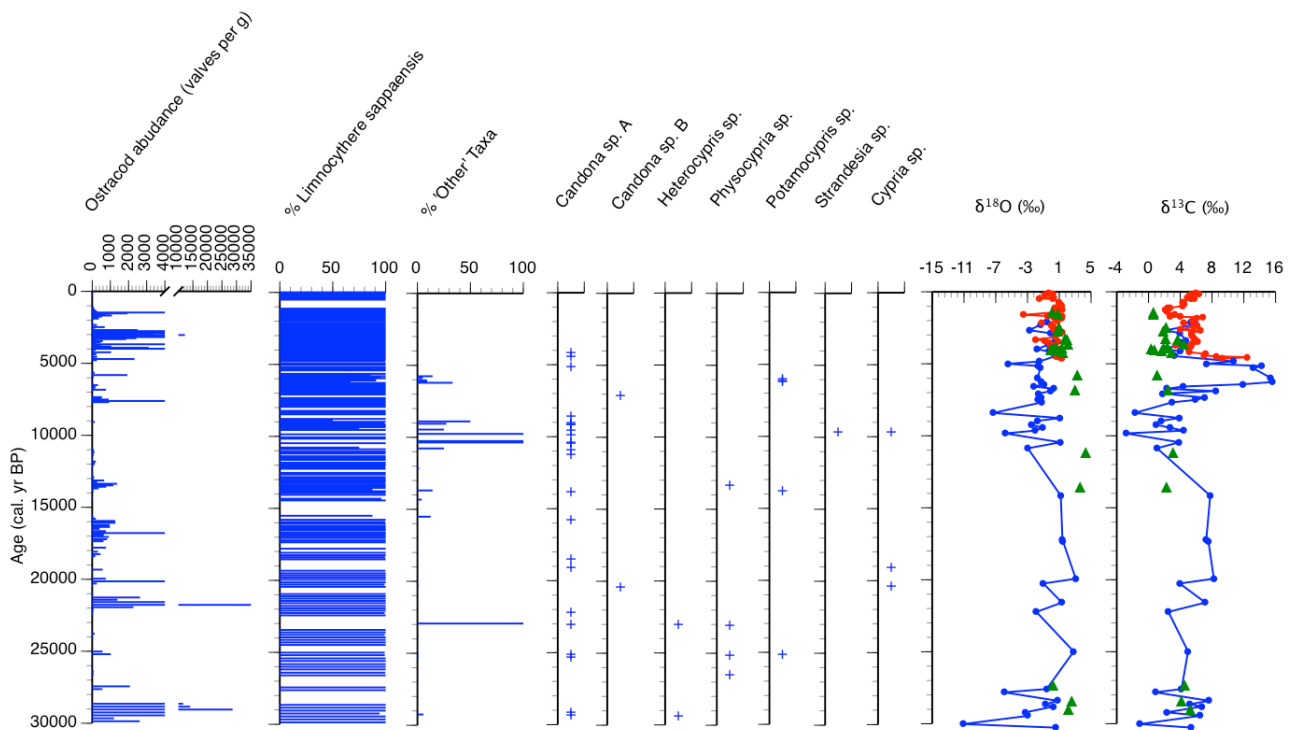
1115

1116 Fig. 2. Age-depth relationships for (a) YC1 (b) YC2, based on radiocarbon dates. The
 1117 datapoints are well described by 3rd order polynomial curves, $AGE = -0.0001Depth^3 +$
 1118 $0.06645Depth^2 + 2.473Depth - 29.23$ for YC1 and, $AGE = -0.000005Depth^3 -$
 1119 $0.0006Depth^2 + 12.23Depth - 109.1$ for YC2 where age is in calendar years BP and depth
 1120 is in cm in both cases. Detailed synchronisation for YC1 and the upper part of YC2 based
 1121 on (c) loss-on-ignition and (d) magnetic susceptibility.



1122

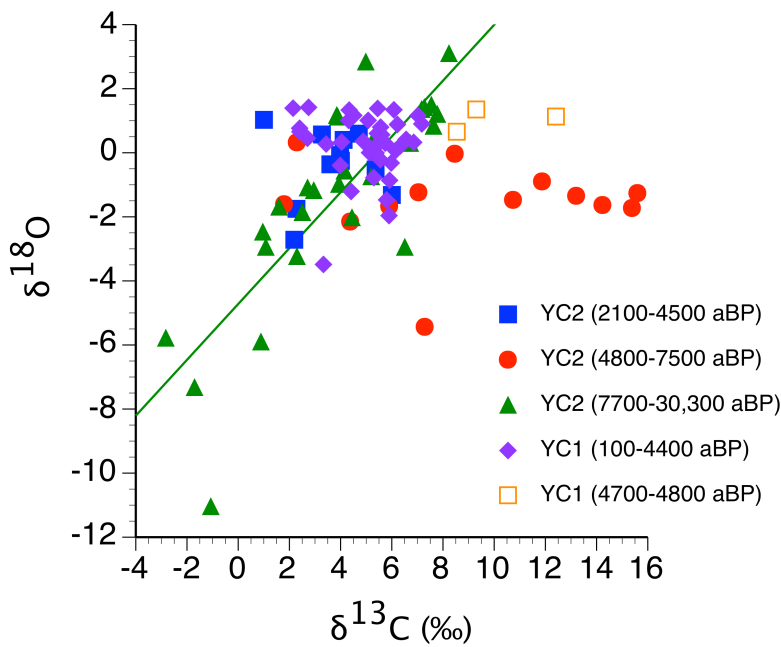
1123 Fig 3. Physical sedimentology and selected elemental geochemical variables for YC1 and
 1124 YC2, plotted as a function of age in calendar years.



1125

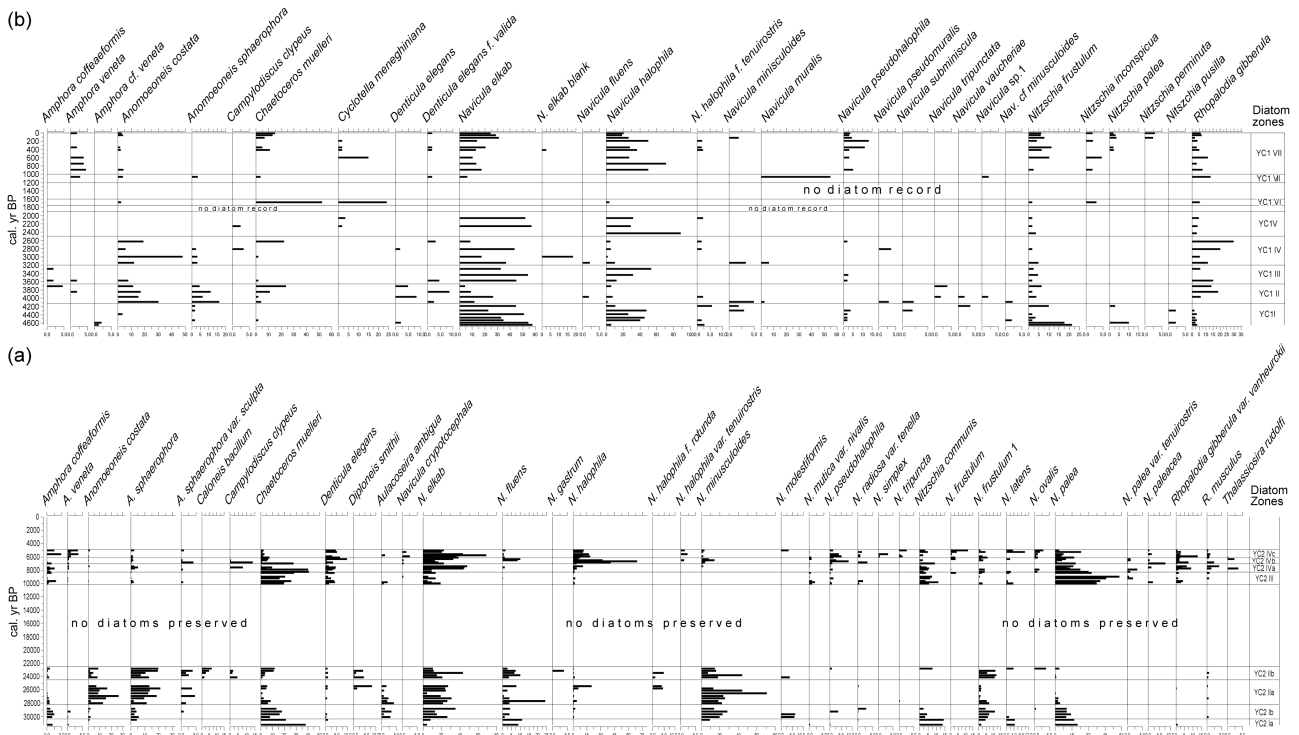
1126 Fig. 4. Ostracod assemblages for YC2 and stable isotopes: endogenic carbonate for YC1
 1127 and YC2 and ostracod shells (triangles) for YC2). The 'other taxa' percentage curve
 1128 includes all taxa except *Limnocythere sappaensis*.

1129



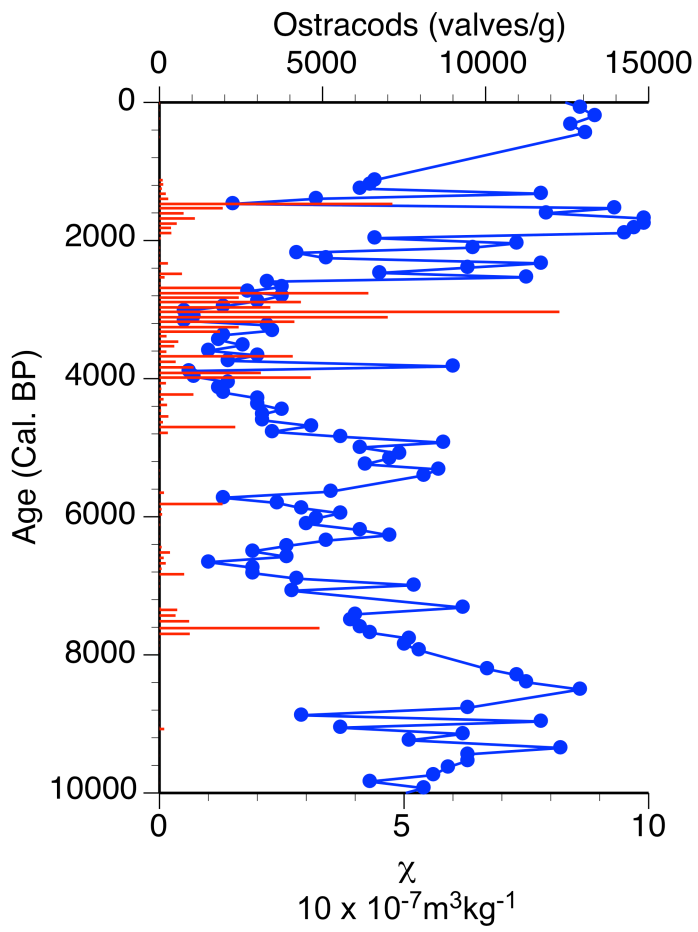
1130

1131 Fig. 5. Covariance of $\delta^{18}\text{O}_{\text{carb}}$ and $\delta^{13}\text{C}_{\text{carb}}$ values for YC1 and YC2. For the interval YC2
 1132 7700-30,300 aBP only, there is significant covariance between $\delta^{18}\text{O}_{\text{carb}}$ and $\delta^{13}\text{C}_{\text{carb}}$ values
 1133 ($R^2 = 0.68$).



1134

1135 Fig. 6. Diatom abundance (%) for (a) YC2 and (b) YC1. Only taxa present at > 2% and in
 1136 more than one sample are plotted.



1137

1138 Fig. 7. Ostracod abundance and magnetic susceptibility for the last 10,000 years in core

1139 YC2.

1140

1141

1142

1143

1144

1145

1146

1147

1148

1149

1150 **Tables**1151 **Table 1. Radiocarbon dates from cores YC1 and YC2.****Table 1. Radiocarbon dates from cores YC1 and YC2**

Core	Depth (cm)	Date Type	Lab number	Radiocarbon age (yr)	Error (yr)	Cal age range (yr) (95 % confidence intervals)		Material	Notes
YC1	44-46	AMS	OxA-1963	875	90	670	951	carbonate	omitted from age model
YC1	74-75	AMS	OxA-1964	570	80	500	673	carbonate	
YC1	122-123	AMS	OxA-1965	900	60	705	927	carbonate	
YC1	157-158	AMS	OxA-1966	1570	80	1307	1680	carbonate	
YC1	194-195	AMS	OxA-1967	2540	60	2383	2759	carbonate	
YC1	250-255	AMS	RIDDL-62	2840	120	2751	3323	carbonate	
YC1	291-292	AMS	OxA-1968	3320	90	3372	3824	carbonate	
YC1	380-385	AMS	RIDDL-63	4100	200	4084	5278	carbonate	
YC2	129-130	AMS	AA13908	860	50	689	908	bulk organic carbon	
YC2	216-217	AMS	AA13907	2125	50	1955	2306	bulk organic carbon	
YC2	321-322	AMS	AA13906	3040	70	3008	3391	bulk organic carbon	
YC2	430-440	Radiometric	SRR-5189	5410	50	6018	6300	bulk organic carbon	
YC2	537-547	Radiometric	SRR-5190	6925	45	7670	7911	bulk organic carbon	
YC2	592-602	Radiometric	2815-Ors	6340	140	6939	7552	bulk organic carbon	omitted from age model
YC2	622-632	Radiometric	SRR-5191	8055	50	8730	9120	bulk organic carbon	
YC2	728-738	Radiometric	2844-Ors	7570	188	8001	8967	bulk organic carbon	omitted from age model
YC2	761-762	AMS	AA13905	9105	80	9969	10511	bulk organic carbon	
YC2	953-954	AMS	AA13904	12865	105	15085	15728	bulk organic carbon	
YC2	1029-1039	Radiometric	2812-Ors	7100	1200	5752	11244	carbonate	omitted from age model
YC2	1093-1094	AMS	AA13903	14705	105	17617	18165	bulk organic carbon	
YC2	1130-1140	Radiometric	2869-Ors	18180	980	19938	24375	bulk organic carbon	
YC2	1190-1200	Radiometric	SRR-5192	19880	75	23676	24160	bulk organic carbon	
YC2	1250-1260	Radiometric	SRR-5193	17275	90	20577	21103	bulk organic carbon	omitted from age model
YC2	1413-1423	AMS	AA16907	26590	280	30308	31189	bulk organic carbon	

1152

1153

1154

1155

1156

1157

1158

1159

1160

1161

1162

1163

1164

1165

1166 Table 2. Summary of climatic and environmental changes at La Piscina de Yuriria over the
 1167 past 30,000 years

Table 2. Summary of climatic and environmental changes at La Piscina de Yuriria over the past 30,000 years

Age Range (cal. aBP)	Climatic and environmental conditions	Key evidence
0-4,500	Lower effective moisture under drier climate regime but with short-lived wetter intervals	Oxygen isotopes
	Saline -alkaline lake	Ostracods, diatoms
	Transient anthropogenically-induced inwash events associated with catchment instability	Elemental geochemistry and magnetic susceptibility
4,500-8,000	Reduced effective moisture leading to enhanced evaporative enrichment under drier climate	Oxygen isotopes
	Saline - alkaline lake with nutrient enrichment and short-lived fresher interval	Ostracods, diatoms
	Intense methane formation	Carbon isotopes
	Climatically-controlled inwash event during wet intervals	Elemental geochemistry and magnetic susceptibility
8,000-11,000	Higher effective moisture, but with evidence of variability under wetter but variable climatic regime	Oxygen isotopes
	Fresher and deeper lake, but eutrophic	Ostracods, diatoms
11,000-14,000	Dry climate, lake dessication	Stratigraphy (presence of desiccation surface)
14,000-25,500	Reduced effective moisture leading to enhanced evaporative enrichment under drier climate	Oxygen isotopes
	Periodic lake desiccation	Stratigraphy (presence of desiccation surface)
	Saline - alkaline lake with short-lived fresher intervals	Ostracods, diatoms
	Shallow eutropic lake with methane formation	Diatoms, carbon isotopes
	Stable catchment with limited inwash	Elemental geochemistry and magnetic susceptibility
27,500-30,000	Rapid shifts between low and high effective moisture under variable dry to wet climatic regime, possibly accompanied by cooler conditions	Oxygen isotopes
	Saline - alkaline lake	Ostracods, diatoms
	Shallow eutropic lake with methane formation	Diatoms, carbon isotopes
	Stable catchment with limited inwash	Elemental geochemistry and magnetic susceptibility

1168

1169

1170

1171 **Supporting online information**

1172 **Table S1. Water Chemistry for La Piscina de Yuriria. Date from Davies (1995) and various**
 1173 **unpublished sources.**

Table S1. Water Chemistry for La Piscina de Yuriria. Date from Davies (1995) and various unpublished sources.

Year	Water depth (m)	Type	pH	EC ^a (µScm ⁻¹)	Alkalinity (Total) (meqL ⁻¹)	Cl (meqL ⁻¹)	SO ₄ (meqL ⁻¹)	K (meqL ⁻¹)	Na (meqL ⁻¹)	Ca (meqL ⁻¹)	Mg (meqL ⁻¹)	TP (µgL ⁻¹)	δ ¹³ C _{DIC} ‰VPDB	δ ¹⁸ O ‰VSMOW	δD ‰VSMOW
1982 (April)	2 (surface)	Lake	11.0	26000	300.0	174.3	29.3	30.7	478.5	0.0	0.0	ND [#]	ND	ND	ND
1982 (April)	2 (at depth)	Lake	NA	23000	326.0	141.5	30.2	24.8	478.5	0.0	0.0	ND	ND	ND	ND
1982 (April)	0.2 (margin)	Lake	11.0	29000	294.0	116.3	29.5	32.1	413.3	0.0	0.0	ND	ND	ND	ND
1982 (April)		Spring	7.5	500	6.2	0.4	1.4	0.6	3.7	1.0	1.3	ND	ND	ND	ND
1982 (April)		Spring	7.0	1100	5.0	1.1	3.6	1.0	9.6	1.1	1.6	ND	ND	ND	ND
1982 (May)	0.2 (margin)	Lake	9.6	27500	333.0	203.0	33.5	32.1	543.7	0.0	0.0	ND	ND	ND	ND
1982 (May)		Spring	7.7	700	8.0	4.2	0.3	0.6	8.9	0.9	1.6	ND	ND	ND	ND
1992 (August)	0.2	Lake	10.5	15620	248.2	117.4	50.0	22.8	298.5	0.3	0.1	ND	-0.2	0.7	-25
1992 (August)		well	6.8	315	3.7	0.4	9.6	0.9	5.7	4.4	3.9	ND	-10.4	-9.2	-69
1992 (August)		spring	8.0	452	7.7	0.4	7.5	2.0	8.4	3.3	3.7	ND	-11.6	-9.1	-69
1997 (March)	shore	Lake	10.2	8130	68.3	27.5	9.2	7.0	95.8	5.9	1.9	ND	ND	ND	ND
2003 (March)	0.2 (margin)	Lake	9.5	1907	20.8	6.2	0.4	1.7	26.3	2.9	2.4	562.0	ND	ND	ND
2004 (July)	0.2 (margin)	Lake	9.6	2910	16.4	16.7	0.8	1.5	163.4*	2.6	0.0	744.5	ND	ND	ND
2003 (March)		Groundwater	8.0	1076	ND	ND	ND	ND	ND	ND	ND	ND	ND	ND	ND

^aElectrical conductivity
[#]ND = not determined
 * possible contamination

1174
 1175

1176

1177

1178

1179

1180

1181

1182

1183

1184

1185

1186

1187

1188

1189

1190 Table S2. Correlation matrices (R^2 values) for correlation amongst selected geochemical
 1191 variables from (a) YC1 (b) YC2, whole core (c) YC2 post 5000 aBP. In each table the null
 1192 hypothesis (H_0) is that there is no statistically-significant relationship between the two
 1193 variables

Table S2. Correlation amongst selected geochemical variables

(a) Core YC1

		K	Fe	Mn	Al
K	R² <i>p-value</i> <i>H0 (5%)</i>	1.			
Fe	R² <i>p-value</i> <i>H0 (5%)</i>	0.65 1.68E-16 <i>rejected</i>	1.		
Mn	R² <i>p-value</i> <i>H0 (5%)</i>	0.68 8.35E-18 <i>rejected</i>	0.77 0.00E+00 <i>rejected</i>	1.	
Al	R² <i>p-value</i> <i>H0 (5%)</i>	0.52 4.76E-12 <i>rejected</i>	0.901 0.00E+00 <i>rejected</i>	0.67 2.46E-17 <i>rejected</i>	1.

(b) Core YC2 - all

		K	Mn	Fe	Al
K	R² <i>p-value</i> <i>H0 (5%)</i>	1.			
Fe	R² <i>p-value</i> <i>H0 (5%)</i>	0.15 0.00001 <i>rejected</i>	1.		
Mn	R² <i>p-value</i> <i>H0 (5%)</i>	0.06 0.00581 <i>rejected</i>	0.45 4.00E-17 <i>rejected</i>	1.	
Al	R² <i>p-value</i> <i>H0 (5%)</i>	0.22 4.32E-08 <i>rejected</i>	0.19 6.67E-07 <i>rejected</i>	0.37 0. <i>rejected</i>	1.

(b) Core YC2 - post 5000 aBP

		K	Mn	Fe	Al
K	R² <i>p-value</i> <i>H0 (5%)</i>	1.			
Fe	R² <i>p-value</i> <i>H0 (5%)</i>	0.61 9.64E-08 <i>rejected</i>	1.		
Mn	R² <i>p-value</i> <i>H0 (5%)</i>	0.49 5.96E-06 <i>rejected</i>	0.75 7.15E-11 <i>rejected</i>	1.	
Al	R² <i>p-value</i> <i>H0 (5%)</i>	0.59 2.00E-07 <i>rejected</i>	0.71 9.10E-10 <i>rejected</i>	0.8 1.67E-12 <i>rejected</i>	1.

1194

1195

1196

1197